



**ADAPTIVE MODULATION CODING MIMO-OFDM SPATIAL
MULTIPLEXING BASED BROADBAND POWERLINE
COMMUNICATION**

**A THESIS SUBMITTED TO
THE GRADUATE SCHOOL OF NATURAL AND APPLIED SCIENCES
OF
GAZI UNIVERSITY**

**BY
Güray KARAARSLAN**

**IN PARTIAL FULFILLMENT OF THE REQUIREMENTS
FOR
THE DEGREE OF MASTER OF SCIENCE
IN
ELECTRICAL ELECTRONICS ENGINEERING**

FEBRUARY 2018

The thesis study titled "ADAPTIVE MODULATION CODING MIMO-OFDM SPATIAL MULTIPLEXING BASED BROADBAND POWERLINE COMMUNICATION" is submitted by Güray KARAARSLAN in partial fulfillment of the requirements for the degree of Master of Science in the Department of Electrical Electronics Engineering, Gazi University by the following committee.

Supervisor: Assoc. Prof. Dr. Özgür ERTUĞ

Electrical and Electronics Engineering, Gazi University

I certify that this thesis is a graduate thesis in terms of quality and content

Chairman: Prof. Dr. Erkan AFACAN

Electrical and Electronics Engineering, Gazi University

I certify that this thesis is a graduate thesis in terms of quality and content

Member: Assoc. Prof. Dr. Emre AKTAŞ

Electrical and Electronics Engineering, Hacettepe University

I certify that this thesis is a graduate thesis in terms of quality and content

Date: 23/02/2018

I certify that this thesis, accepted by the committee, meets the requirements for being a Master of Science Thesis.

.....

Prof. Dr. Sena YAŞYERLİ

Dean of Graduate School of Natural and Applied Sciences

ETHICAL STATEMENT

I hereby declare that in this thesis study I prepared in accordance with thesis writing rules of Gazi University Graduate School of Natural and Applied Sciences;

- All data, information and documents presented in this thesis have been obtained within the scope of academic rules and ethical conduct,
- All information, documents, assessments and results have been presented in accordance with scientific ethical conduct and moral rules,
- All material used in this thesis that are not original to this work have been fully cited and referenced,
- No change has been made in the data used,
- The work presented in this thesis is original,

or else, I admit all loss of rights to be incurred against me.

Güray KARAARSLAN

23/02/2018

UYARLAMALI MODÜLASYON KODLAMALI MIMO-OFDM UZAYSAL
ÇOKLAMA BAZLI GENİŞ BANTTA GÜÇ HATTI ÜZERİNDEN HABERLEŞME

(Yüksek Lisans Tezi)

Güray KARAARSLAN

GAZİ ÜNİVERSİTESİ
FEN BİLİMLERİ ENSTİTÜSÜ

Şubat 2018

ÖZET

Güç hattı şebekeleri, geniş bantta haberleşme sistemi kurmak için mükemmel bir alternatif oluşturmaktadır. Fakat güç hattı haberleşme kanalı, yapısı nedeniyle, çok yollu sönümlenme ve dürtü gürültüsü gibi bozucu etkilere sahiptir. Bu çalışmada, uyarlamalı modülasyon kodlama tekniği kullanılarak; bu bozucu etkilerin giderilmesi ve bit-hata-oranı performansının artırılması üzerine çalışmalar yapılmıştır. Bunlara ek olarak, güç hattı sisteminin birçok kabloyu ihtiva etmesi ile çok-giriş çok-çıkış haberleşme sisteminin kurulabilmesine olanak sağlanmaktadır. Bu çalışmada, tek-giriş tek-çıkış, 2x2 ve 3x3 çok-giriş çok-çıkış haberleşme sistemleri kurulmuş ve modülasyon şeması olarak QPSK, 16-QAM ve 64-QAM şemaları seçilmiştir. Kanal kodlama olarak, turbo kodlayıcı tekniği kullanılmış ve kodlama oranı olarak da 1/2 ve 3/4 oranları seçilmiştir. Sonuç olarak, çok yollu sönümlenme ve dürtü gürültüsüne sahip güç hattı haberleşme kanalında, uyarlamalı modülasyon kodlama tekniğinin bit-hata-oranı performansının sabit modülasyon ve kodlamaya göre, geniş bant haberleşmede, daha etkin olduğu hem tek-giriş tek çıkış hem de çok-giriş çok-çıkışlı sistemlerde gösterilmiştir.

Bilim Kodu : 93523

Anahtar Kelimeler : Geniş bantta güç hatları üzerinden haberleşme, MIMO-PLC, uyarlamalı modülasyon kodlamalı, OFDM, dürtü gürültüsü

Sayfa Adedi : 53

Danışman : Doç. Dr. Özgür ERTUĞ

ADAPTIVE MODULATION CODING MIMO-OFDM SPATIAL MULTIPLEXING
BASED BROADBAND POWERLINE COMMUNICATION

(M. Sc. Thesis)

Güray KARAARSLAN

GAZİ UNIVERSITY
GRADUATE SCHOOL OF NATURAL AND APPLIED SCIENCES

February 2018

ABSTRACT

Power-line networks are great candidates for broadband communication systems. However, a power-line channel suffers from multipath effects, and impulsive noise due to harsh environment in the network. This study attempts to overcome these obstacles and increase the-bit-error-rate performance by using adaptive modulation and coding. Additionally, the multiple wires allow the communication via more than one channel. Thus, multiple-input multiple-output communication system can be utilized in the powerline. In this study QPSK, 16-QAM, and 64-QAM schemes and turbo coding at 1/2 and 3/4 coding rates; SISO, 2x2, and 3x3 MIMO channels are used. As a result, it is observed that adaptive modulation and coding techniques perform better than fixed modulation schemes under multipath fading and impulsive noise both for SISO, and MIMO channels in broadband power-line communication. Additionally, it is found that the bit-error-rate performance is increased by using spatial multiplexing technique in powerline communication.

Science Code : 93523

Key Words : Broadband powerline communication (BPLC), MIMO-PLC, adaptive modulation and coding, OFDM, impulsive noise

Page Number : 53

Supervisor : Assoc. Prof. Dr. Özgür ERTUĞ

ACKNOWLEDGEMENT

First and for most, I would like to express my sincere thanks to my supervisor Assoc. Prof. Özgür ERTUĞ for his constant guidance, invaluable support and advice throughout the writing process of this thesis.

I would like to convey my gratefulness to all faculty and staff in Electrical and Electronics Engineering Department at Erciyes University for their priceless guidance and helps during my undergraduate years.

I would like to acknowledge the constant support and love provided by my mother Şenay KARAARSLAN, and my father Erkan KARAARSLAN. I would like to thank my mother in-law Gülizar VARLI, and my father in-law Şerafettin VARLI for their motivation and supports.

I would like to state my appreciativeness to my sister in-law Güliz VARLI for her helps and never ending positive energy.

I would like to give thanks to my decedent sister Eray KARAARSLAN. Her special memories will live on forever in my heart.

And lastly, I would like to give my special thanks to my beloved wife, Gül VARLI KARAARSLAN for her unceasing help, support and unwavering love.

CONTENTS

	Page
ÖZET	iv
ABSTRACT	v
ACKNOWLEDGEMENT	vi
CONTENTS	vii
LIST OF TABLES	ix
LIST OF FIGURES	x
ABBREVIATIONS	xii
1. INTRODUCTION	1
2. POWERLINE SYSTEM MODEL	5
2.1. Powerline Channel Models	5
2.1.1. Multipath model	6
2.2. Noise in Powerline Channel	11
2.2.1. Middleton class-A noise model	13
3. OFDM SYSTEM MODEL AND ADAPTIVE MODULATION AND CODING....	15
3.1. OFDM System Model	17
3.1.1. Cyclic prefix	20
3.1.2. Quadrature amplitude modulation/OFDM	20
3.2. Link Adaptation (Adaptive Modulation and Coding)	23
3.2.1. Channel estimation	25
3.2.2. Turbo coding	27
3.2.3. Turbo decoder	31
4. MULTIPLE-INPUT MULTIPLE-OUTPUT POWERLINE COMMUNICATIONS	35

	Page
4.1. MIMO-PLC Channel Model	36
5. SIMULATION RESULTS AND DISCUSSIONS.....	41
6. CONCLUSION	47
REFERENCES	49
RESUME.....	53

LIST OF TABLES

Table	Page
Table 2.1. Parameters of 4-path model	9
Table 2.2. Parameters of 15-path model	10
Table 4.1. The statistical CTF parameters	38
Table 5.1. SNR thresholds modulation coding table	42

LIST OF FIGURES

Figure	Page
Figure 1.1. The conventional power grid.....	1
Figure 2.1. Multipath signal propagation with one tap.....	6
Figure 2.2. Amplitude response of 4-path channel.....	10
Figure 2.3. Amplitude response of 15-path channel.....	11
Figure 2.4. Noise scenario in the powerline channel.....	13
Figure 3.1. OFDM-AMC system model.....	16
Figure 3.2. The comparison of the bandwidth gain between FDM and OFDM	17
Figure 3.3. ISI between data blocks in channel output.....	20
Figure 3.4. QAM modulator structure	21
Figure 3.5. M=8 PAM-PSK signal space diagram.....	22
Figure 3.6. 4-QAM and 16-QAM constellations	23
Figure 3.7. AMC system model	24
Figure 3.8. MMSE channel estimation	26
Figure 3.9. A turbo coder with 1/3 coding rate	28
Figure 3.10. Convolutional coder, G[111;101]	29
Figure 3.11. Recursive systematic convolutional coder, G[111;101]	29
Figure 3.12. The interleaver and the deinterleaver operations.....	30
Figure 3.13. Turbo decode.....	31
Figure 4.1. MIMO-PLC channel model.....	36
Figure 4.2. Example of MIMO-PLC channel transfer function depends on the purposed statistical MIMO model (Tx: D1 only)	39
Figure 5.1. 4-path fading channel BER performance	42
Figure 5.2. 15-path fading channel BER performance	43

Figure	Page
Figure 5.3. BER performance of 2x2 MIMO-PLC	44
Figure 5.4. BER performance of 3x3 MIMO-PLC	45

ABBREVIATIONS

The symbols and abbreviations used in this study are presented with their descriptions below.

Symbols	Descriptions
A	Impulsive index
A(t)	Amplitude of signal
d_i	Length of path
f_c	Carrier frequency
g_n	Weighting factor
H(f)	Channel transfer function
h_{nm}(f)	Channel coefficients
k	Attenuation parameter
n	Noise
s	Signal
t_b	Transmission factor
Z	Impedance
γ	Reflection factor
σ	Variance
τ_i	Path delay
φ(t)	Phase of signal
Abbreviations	Descriptions
AMC	Adaptive modulation and coding
BCJR	Bahl, Cocke, Jelinek and Raviv
BER	Bit-error-rate
BPLC	Broadband powerline communication
CP	Cyclic prefix
CQI	Channel quality information
CSI	Channel state information
CTF	Channel transfer function

Abbreviations**Descriptions**

DC	Direct current
FDM	Frequency division multiplexing
FEC	Forward error correction
FFT	Fast Fourier transform
GIS	Gaussian to impulsive noise
HDTV	High definition television
ICI	Inter-carrier interference
IFFT	Inverse Fast Fourier transform
ISI	Inter-symbol interference
LOS	Line-of-sight
MAP	Maximum a posteriori probability
MIMO	Multiple-input multiple-output
MMSE	Minimum mean square error
N	Neutral
OFDM	Orthogonal frequency-division multiplexing
P	Phase
PAM	Pulse amplitude modulation
PDF	Probability density function
PE	Protective earth
PLC	Powerline communication
PSD	Power spectral density
PSK	Phase shift keying
QPSK	Quadrature phase shift keying
RSC	Recursive systematic convolutional encoder
SISO	Single-input single-output
SNR	Signal-to-noise ratio
SSB	Single-side band

1. INTRODUCTION

Electric power is an essential type of energy that is commonly used in various fields. Electric power is supplied to users by powerlines. Powerlines cover a vast domain since they carry electrical power to residential areas.

Powerlines consist of power plants, transmission and distribution lines. They are classified in accordance with the voltage level that is transmitted from the power plants to the last user in the line. These classes are divided into three main sorts namely, high, medium, and followed by low voltage powerlines.

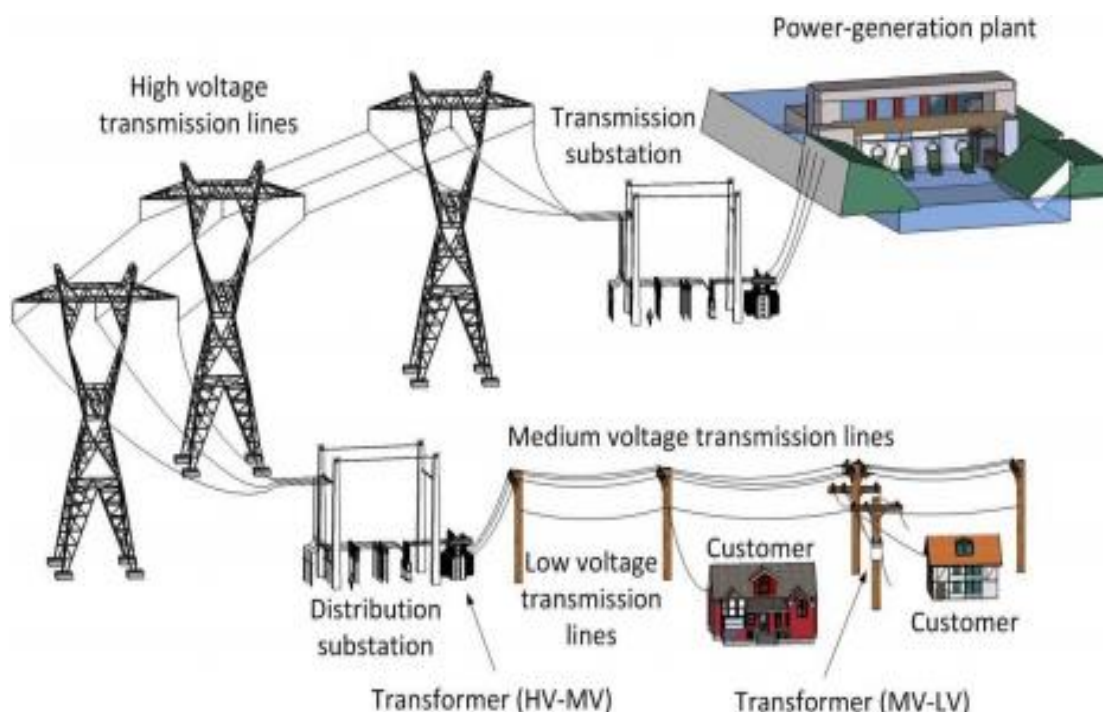


Figure 1.1. The conventional power grid [11]

The transmission line that is lined between the power plants and high/medium voltage transformer (substation) is called high voltage (380/110 kV) powerline. High voltage line is preferred to be used in the long-distance transmission of energy and supplied through aerial powerlines.

Medium voltage powerline (10/30 kV) is used to supply the necessary energy demanded in metropolitan cities and industrial zones. It can be supplied through either aerial powerlines or underground powerlines.

Low voltage power lines (220/380 V) are often short lines that supply energy to the last users of the line. They generally supply energy through underground lines in the city centers and through aerial powerlines in the suburban areas.

When the energy reaches the building, it is distributed to each room through three parallel cables that are categorized as phase, neutral, and ground. The line in the room ends with a plug socket. This system in the buildings creates a natural local web. Although the central aim of this line scheme is to provide energy, in many cases, it is proved to be an efficient method to use for communication systems [16].

Accordingly, in the last few decades, there is a constantly growing interest to operate the powerline infrastructures for using as a communication system purposes. The most significant advantage of the power-line communication (PLC) is quite apparent since the existing power-line networks are currently available in any zone. Moreover, broadband powerline communication (BPLC), which empowers a reliable high data rate transmission over the powerline channels, can be obtained at a low cost as it does not need any further substructure [38]. Furthermore, there has been a widening attention to numerous broadband powerline communication implementations including; broadband internet, home networks, HDTV, telephone, and fax services. However, the powerlines have been planned for conducting the electrical power without considering communication. Thereby, in such a system, there happens to be a set of standard channel distortions along with impulsive noise and multipath fading owing to the changing load on the power line. Obtaining such a feature, a power-line communication system is quite similar to wireless communication systems.

The focus of this study covers adaptive modulation and coding MIMO-OFDM technique in the broadband powerline communication system, and the improvement in bit-error-rate performance is observed.

To achieve broadband transmission, the multicarrier modulation, such as OFDM is utilized. OFDM is also a useful technique for BPLC. The study indicates that OFDM system is preferable under BPLC channel conditions compared to a single carrier.

In order to increase BER performance, in this study QPSK, 16-QAM, and 64-QAM schemes and turbo coding at 1/2 and 3/4 coding rates are used. As a result, it is observed that adaptive modulation and coding technique performs better than fixed modulation schemes powerline communication channel conditions.

Furthermore, in this thesis, different types of multiple-input and multiple-output systems are utilized in order to improve BER performance. Upon considering three-phase and neutral wires in the powerlines as the transmitter antennas and the receiver antennas, spatial multiplexing is installed and the changes in BER performance are observed and recorded. In this thesis, SISO, 2x2 MIMO, and 3x3 MIMO communication systems are installed and adaptive modulation and coding as well as BER performance are acquired for each one and outcomes are compared.

To evaluate the performance of BPLC network, proper channel characteristics should be modelled. In the literature, there are different models present for PLC channel such as Philipps model [15], the Zimmermann and Dosteret model [40], and the Anatory et al. [1] model. In this study, we implement the Zimmermann's multipath channel model to exhibit the power-line multipath fading [40].

Additionally, the noise, added by the channel, distorts the communication signals. The noise in the powerline communication system may be split into two branches; including background noise and impulsive noise. Similar to the conditions of channel models, there are some different forms of noise models for modeling impulsive noise and background noise in the literature. In this study, we implement one of the most popular noise model which is Middleton class A [41] noise model.

This study includes five chapters. The information and the mathematical equations of the powerline system, the channel models, and types of the noise are given in Chapter 2. The modulation schemes, adaptive modulation and coding technique, channel estimation, and turbo coding/decoding are examined in Chapter 3. Multiple-input multiple-output (MIMO) system, MIMO-PLC system, and MIMO-PLC channel model are reviewed under the Chapter 4. Simulation results and discussions are given in Chapter 5. Finally, the conclusion is given in Chapter 6.

2. POWERLINE SYSTEM MODEL

In the last few decades, there is a growing attention to operate the powerline network for communication. The most significant advantage of the power-line communication (PLC) is that quite apparent since existing power-line networks are currently available in any zone. There are a lot of studies over powerline communication systems [21], [16], [18].

We can categorize the powerline communication system under two main titles:

1. Powerline Channel Models
2. Powerline Noise Models

2.1. Powerline Channel Models

There has been an expanding interest in numerous BPLC implementations including; broadband internet, smart grid applications, home networks, HDTV, telephone, and fax services. However, the powerlines have been planned for conducting the electrical power without considering high-speed communication. Thereby, in such a system, there are several major channel distortions along with impulsive noise and multipath fading owing to the changing load on the powerline.

The data signals in powerline network do not track a single path; rather they follow a multipath in line with the channel conditions. Although the powerline communication is a wire-based communication system, depending upon the channel conditions in the system, is very similar to the wireless communication system.

In the literature, there are different models present for PLC channels such as Philipps model [15], the Zimmermann and Dosteret model [40], and the Anatory et al. [1]. However, existing models are based on two main approaches to define the transfer function of powerlines that are namely, time domain and frequency domain [18]. Time-domain models are, in general, based on measurement tests and averaging of the acquired results. Nevertheless, frequency domain models are based on the deterministic approach. As the time-domain approach, the multipath channel model is reviewed in the next title.

2.1.1. Multipath model

“Opposite to the telephone copper loop, the powerline “local loop access network” does not consist of point-to-point connections between substations and customer’s premises, but represents a line bus” [40]. Due to this characteristic of the powerline system, the signal propagation does not occur as merely a direct line-of-sight (LOS) path from the transmitter to the receiver; hence additional paths should be also taken into account.

The multipath channel model is illustrated as a simple example in Fig 2.1. The link contains only one branch and pieces (1), (2), and (3) with the characteristic impedances Z_{L1} , Z_{L2} , and Z_{L3} and the lengths l_1 , l_2 , and l_3 respectively.

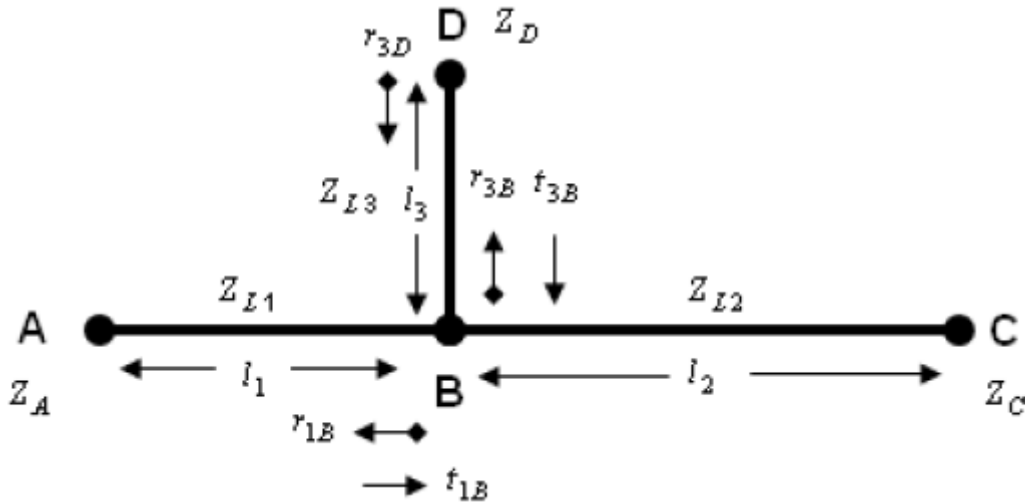


Figure 2.1. Multipath signal propagation with one tap

To simplify the analysis of the system, A and C are assumed to be matched, so it means $Z_A=Z_{L1}$ and $Z_C=Z_{L2}$. The remaining two points B and D represent the reflection points. To end the transmission line accurately, the load should be connected to the transmission line which has equal impedance with the characteristic impedance of the line, which is Z_L . Thus, all the signals can be transmitted. It is assumed that point D belongs to the branch, which has length l_3 , does not end correctly.

The reflection factors for the point B and D are denoted as:

$$\gamma_{1B} = \frac{(Z_{L2} || Z_{L3}) - Z_{L1}}{(Z_{L2} || Z_{L3}) + Z_{L1}}, \quad (2.1)$$

$$\gamma_{3D} = \frac{Z_D - Z_{L3}}{Z_D + Z_{L3}}, \quad (2.2)$$

$$\gamma_{3B} = \frac{(Z_{L2} || Z_{L1}) - Z_{L3}}{(Z_{L2} || Z_{L1}) + Z_{L3}}. \quad (2.3)$$

The transmission factors can be denoted as:

$$t_{1B} = 1 - |\gamma_{1B}|, \quad (2.4)$$

$$t_{3B} = 1 - |\gamma_{3B}|. \quad (2.5)$$

The reflection and the transmission factors represented the transmitted and reflected signals' weightings.

Under these assumptions, principally an unlimited number of propagation paths are probable, as a result of multiple reflections:

$$(1) A \rightarrow B$$

$$(2) A \rightarrow B \rightarrow D \rightarrow B \rightarrow C$$

.

$$(N) A \rightarrow B \rightarrow (D \rightarrow B)^{N-1} \rightarrow C \quad (N \rightarrow \infty)$$

The analysis of the given communication system from the transmitter at point *A* to the receiver at point *B* shows that some part of the signal, transmitted from the point *A*, reflects back while some part of the signal moves into the point *C* and *D*. The signal that reached to the point *D* reflects to the point *B*. While some part of the signal, which is reaching to the point *B*, moves through the point *A* and *C*, some part of the signal reflects back. The signals reaching point *A* and *C* are terminated. However, the signals between the point *B* and *D* enter an infinite loop.

All the paths have its weighting factor g_i which represents the multiplication of the transmission and the reflection factors through the path. The impedance occurs due to the parallel connections of two or more than two cables at the output cable of the transmitter, lower than the characteristic impedance of the transmitter. This causes to mismatch of impedances at the point of connection; so, the transmission and reflection factors are generally less than one or equal to one.

$$g_1 = t_{1B}$$

$$g_1 = t_{1B} \cdot \gamma_{3D} \cdot t_{3B}$$

.

.

$$g_N = t_{1B} \cdot \gamma_{3D} \cdot (\gamma_{3B} \cdot \gamma_{3D})^{N-2} \cdot t_{3B}$$

The unlimited number of propagation paths between the point A and C cause many difficulties over the calculations. In order to simplify the calculations, the propagation path numbers can be restricted to specific numbers. When setting this number, weighting factor g_i should be considered. Signal attenuation increases when the length of propagation path increase and g_i approaches to zero value. By selecting the most dominant N number paths with g_i , multipath channel number is determined. The number of the paths is generally in the range between 5 and 50 [24].

The other factor that affects the signal propagation in the transmission line is the delay, τ_i . "Each path's delay, τ_i , can be calculated with dielectric constant ϵ_r , the velocity of light c_0 , and the lengths of the cables d_i " [40].

$$\tau_i = \frac{d_i \sqrt{\epsilon_r}}{c_0} = \frac{d_i}{V_r}, \quad (2.6)$$

The last factor which affects the transmission line is the attenuation of a power line cable. The attenuation of the signal depends on the frequency and the length of transmission line. The attenuation of the transmission signal is [40]:

$$A(f, d) = e^{-\alpha(f)di}, \quad (2.7)$$

$$\alpha(f) = a_0 + a_1 f^k, \quad (2.8)$$

where a_0 and a_1 are the attenuation parameters and k is an exponent of the attenuation factor [40].

Finally, by merging the aforementioned formulas, the transfer function of multipath channel $H(f)$ can be acquired [10]. The channel transfer function can be formulated as follows:

$$H(f) = \sum_i^N g_i \cdot e^{-(a_0 + a_1 f^k) d_i} \cdot e^{-j2\pi f (d_i/v_p)}, \quad (2.9)$$

where $H(f)$ is the frequency response of the multipath channel, d_i is the length of path, g_i is the weighting factor, k is the attenuation factor, a_0 and a_1 are attenuation parameters.

Equation of $H(f)$ stands for parametric model, explaining the frequency response of multipath fading powerline channel, it covers all significant effects of the transfer properties in the frequency interval from 1 MHz to 20 MHz via minor set of parameters, given in the study [40], and shown in Table 2.1 and Table 2.2. Furthermore, the number of paths, N , makes it possible to control the sensitivity of the model, which is very important for analyzing PLC system performance.

Table 2.1. Parameters of 4-path model [40]

Attenuation Parameters					
$k = 1$		$a_0 = 0$		$a_1 = 7.8 * 10^{-10} \text{ s/m}$	
Path Parameters					
I	g_i	d_i/m	I	g_i	d_i/m
1	0.64	200	3	-0.15	244.8
2	0.38	222.4	4	0.05	267.5

In this study, two different Zimmermann multipath models that are 4-path and 15-path are performed. According to the parameters for those models; the amplitude responses are shown in Fig. 2.2, and Fig. 2.3, respectively.

Table 2.2. Parameters of 15-path model [40]

Attenuation Parameters					
$k = 1$		$a_0 = 0$		$a_1 = 7.8 * 10^{-10} s/m$	
Path Parameters					
I	g_i	d_i/m	I	g_i	d_i/m
1	0.029	90	9	0.071	411
2	0.043	102	10	-0.035	490
3	0.103	113	11	0.065	567
4	-0.058	143	12	-0.055	740
5	-0.045	148	13	0.042	960
6	-0.040	200	14	-0.059	1130
7	0.038	260	15	0.049	1250
8	0.038	322			

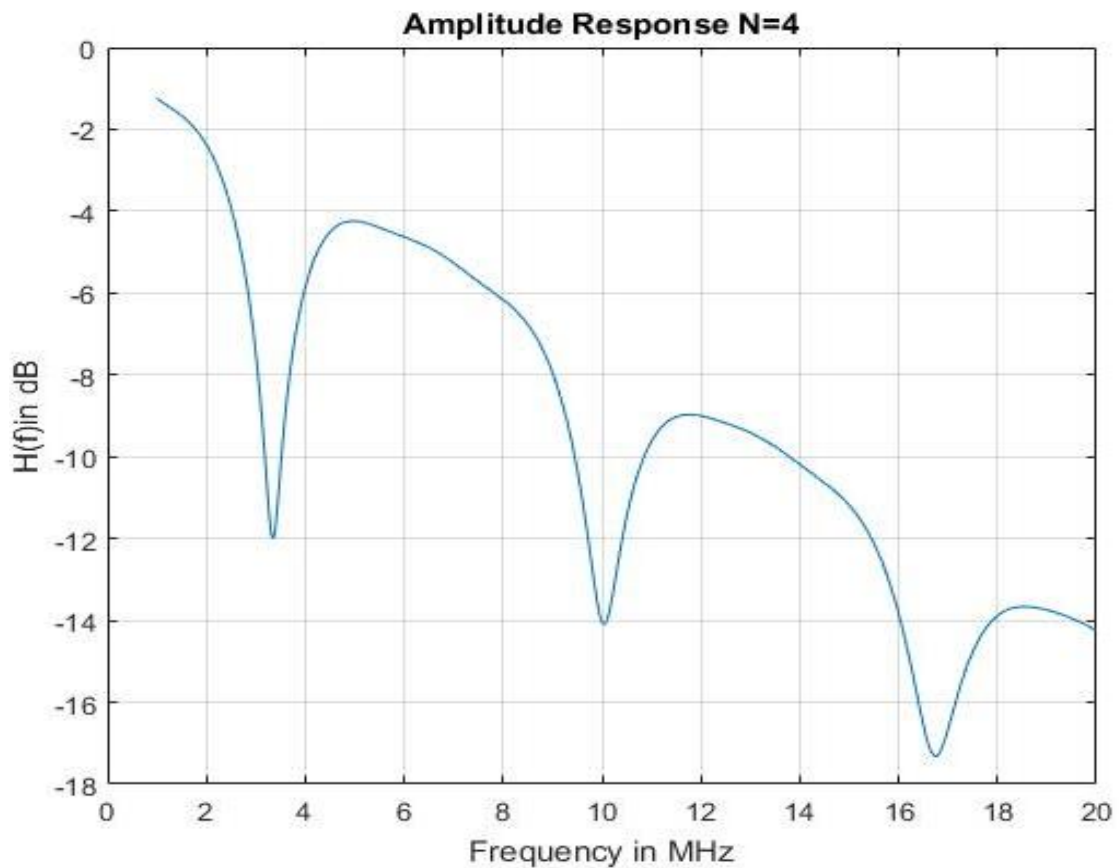


Figure 2.2. Amplitude response of 4-path channel

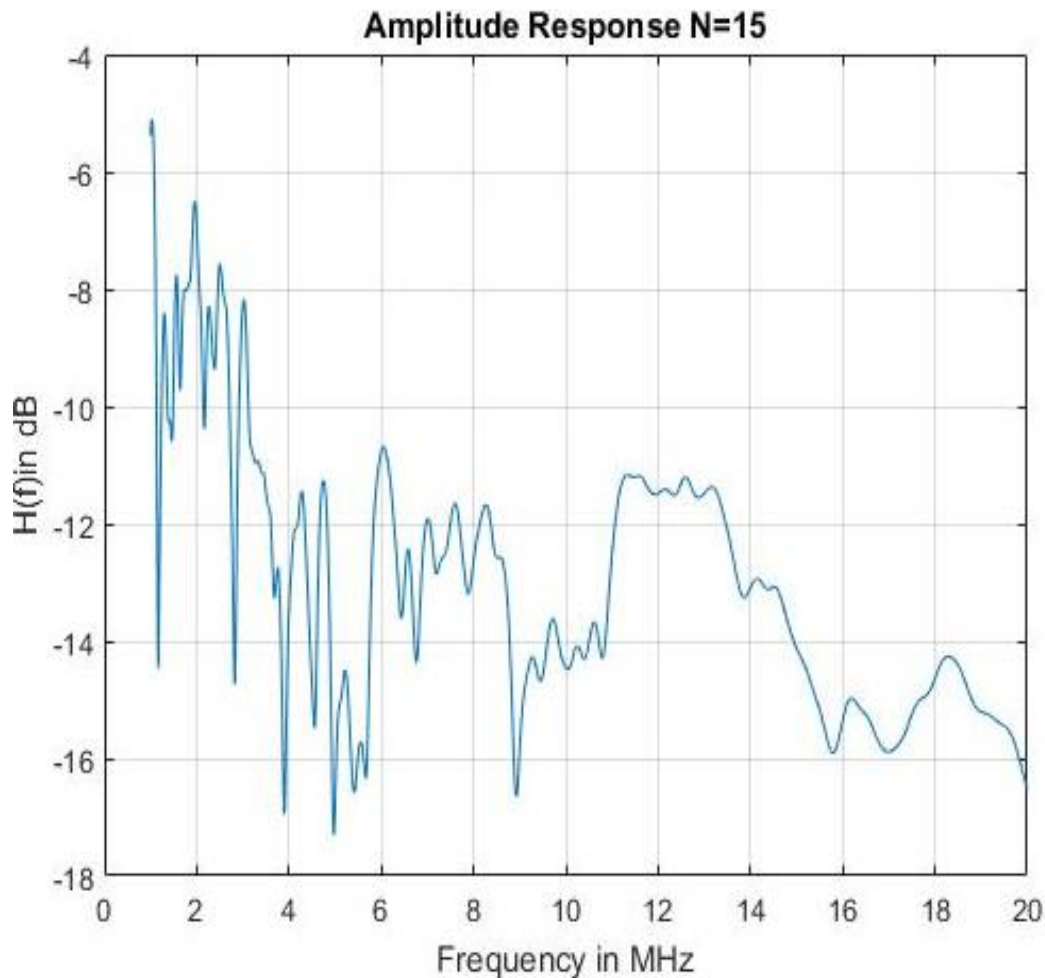


Figure 2.3. Amplitude response of 15-path channel

2.2. Noise in Powerline Channel

In literature, noise in the powerline is calculated by using different mathematical methods. While some of these methods focus on the noise, [22], some others try to model the noise in groups [41], [25].

Middleton developed a model that defines electromagnetic interference statistically and physically. In Middleton's theory, electromagnetic interference is categorized under three main branches. The calculation of the powerline noise, by using "Middleton's Class A noise model" is the most commonly adapted one. "Middleton's class A model" has many parameters which enable to calculate instantaneous powerline noise under a parametric signal formula.

A detailed study [41] lists the power-line noise as follows:

- 1) “*Colored background noise*” with comparatively low power spectral density (PSD) varies with frequency. A summation of various low power noise sources primarily causes this sort of noise. In this respect, the PSD is modified in time with regards to minutes or hours.
- 2) “*Narrow-band noise*” and especially sinusoidal signals that have modulated amplitudes are results of ingress of broadcast stations. The level often changes during the daytime.
- 3) “*Periodic impulsive noise asynchronous to the mains*” frequency with a repetition rate between 50 and 200 kHz, with a discrete line spectrum located in accordance with the impulse repetition rate. Switched power supplies are generally the reason for this sort of noise.
- 4) “*Periodic impulsive noise synchronous to the mains*” frequency with a repetition rate of 50 or 100 Hz. The impulses have short life span lasting around microseconds and their PSD declines with frequency. Power supplies are the reason for this sort of noise especially through switching of rectifier diodes, and this emerges synchronously with the mains cycle.
- 5) “*Asynchronous impulsive noise*” is stimulated by switching transients in the network. The impulses endure from some microseconds to milliseconds and occur randomly. The PSD of this kind of noise is able to attain values more than 50 dB above the background noise.

The features of first two noise types remain constant over long periods of time lasting for seconds, minutes, and may be hours. Therefore, they can be defined as the “background noises”. On the contrary, the last three types can be summarized as “impulsive noise” since their root-mean square (RMS) amplitudes vary rapidly over time (microseconds, milliseconds). Thus, the powerline noise can be considered as the summation of background noise and impulsive noise [40].

In this study, we implement “Middleton’s Class-A impulsive noise model” [39] since it satisfies all the fundamental requirements in noise modeling.

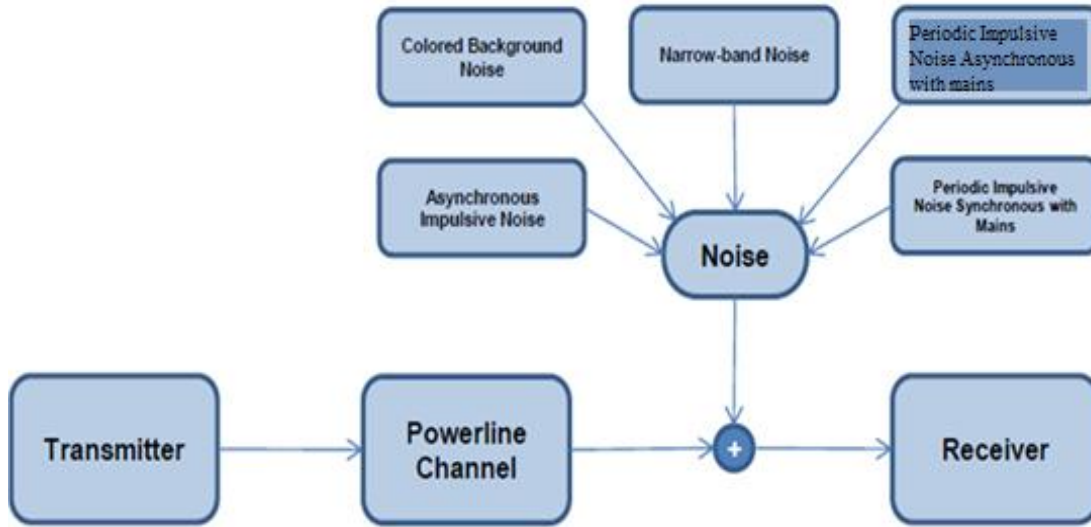


Figure 2.4. Noise scenario in the powerline channel

2.2.1. Middleton class-A noise model

Middleton proposes a noise model which takes the general characteristics of the physical environment. Thus, the interfering sources which have different powers and volumes can be expressed. Middleton Class A model examines the mixture of these sources as a physical scenario. While Middleton expresses Class A summation model, he uses several mathematical parameters. The estimation of these parameters provides a convenient method to express various types of noise.

The Middleton Class A model can be expressed as follows:

$$n(t) = n_I(t) \cos(2\pi f_c t) - n_Q(t) \sin(2\pi f_c t), \quad (2.10)$$

where f_c is the frequency of the noise; n_I , and n_Q are the components of narrow-band noise. According to Middleton's class-A noise model, the mixture of background and impulsive noise is a series of independent and identically distributed complex random variables. The model with probability density function (PDF) is defined as [7]:

$$p_z(z) = \sum_{m=0}^{\infty} \frac{\alpha_m}{2\pi\sigma_m^2} \exp\left(-\frac{z^2}{2\sigma_m^2}\right), \quad (2.11)$$

$$\alpha_m = e^{-A} \frac{A^m}{m!}, \quad (2.12)$$

$$\sigma_m^2 = \sigma_g^2 \frac{\left(\frac{m}{A}\right) + \Gamma}{\Gamma}, \quad (2.13)$$

$$\sigma_z^2 = E\{z^2\} = \frac{e^{-A}\sigma_g^2}{\Gamma} \sum_{m=0}^{\infty} \frac{A^m}{m!} \left(\frac{m}{A} + \Gamma\right), \quad (2.14)$$

where m is the number of impulsive noise sources, A is an impulsive index (If A is increased, the impulsiveness becomes weaker, and the noise approaches to Gaussian noise), Γ is the Gaussian to impulsive noise ratio (GIR), and $\Gamma = \sigma_g^2 / \sigma_m^2$ where σ_g^2 is the variance of Gaussian noise components, and σ_m^2 is the impulsive noise power. Finally, σ_z^2 represents the variance of Middleton's Class a noise.

According to Middleton's model, different noise sources' emission their random processes, are symbolized with $n_i(t, \theta)$, to the channel. This process is modelled with Poisson distribution. The summation of the noises with Poisson distributed and Gauss distributed expresses the total noise in the channel as shown in Eq. 2.15.

$$n(t) = n_G(t) + \sum_i n_i(t, \theta). \quad (2.15)$$

3. OFDM SYSTEM MODEL AND ADAPTIVE MODULATION AND CODING

Orthogonal Frequency Division Multiplexing (OFDM) is a very efficient modulation technique, which is widely used in broadband communication, to handle with the inter-symbol interference (ISI), and it also reduces the results of multipath [6]. It presents a perfect spectral efficiency which is necessary for a channel with barely restricted spectral resources such as PLC. OFDM also shows better performance in the presence of impulsive noise conditions than single-carrier modulation techniques. Moreover, the most important property of OFDM is its adaptability. According to the PLC channel terms, several parameters, such as; transmit power, data rate, code rate, and constellation size can be adjusted to optimize the efficiency of the system based on the channel conditions through adaptive modulation algorithms.

In order to improve the performance of BPLC system, adaptive modulation coding (AMC) can be utilized. AMC technique allows controlling each sub-channel's constellation size depending on the channel conditions. In AMC, some parameters can be controlled such as data rate, instantaneous BER, channel code/scheme, and constellation size. To control those parameters, AMC requires up-to-date channel quality information (CQI) at the transmitter. This information shows the signal condition in the link from the transmitter to receiver end.

Channel quality information (CQI) should be estimated at the receiver. In this study, the minimum mean square error (MMSE) estimator [6] is utilized to obtain CQI at the receiver. Once the MMSE estimator evaluates the instantaneous SNR in the channel, the mode selector gives feedback to the transmitter in order to adapt constellation scheme and coding rate. The coding rate and modulation scheme is adjusted according to SNR thresholds are acquired from the performance of each scheme in the PLC channel possessing target BER of 0.001. Likewise, the receiver should also be given feedback about demodulation and decoding parameters which are required to be used for the following frame. The diagram of the OFDM-AMC system model is shown in Fig. 3.1.

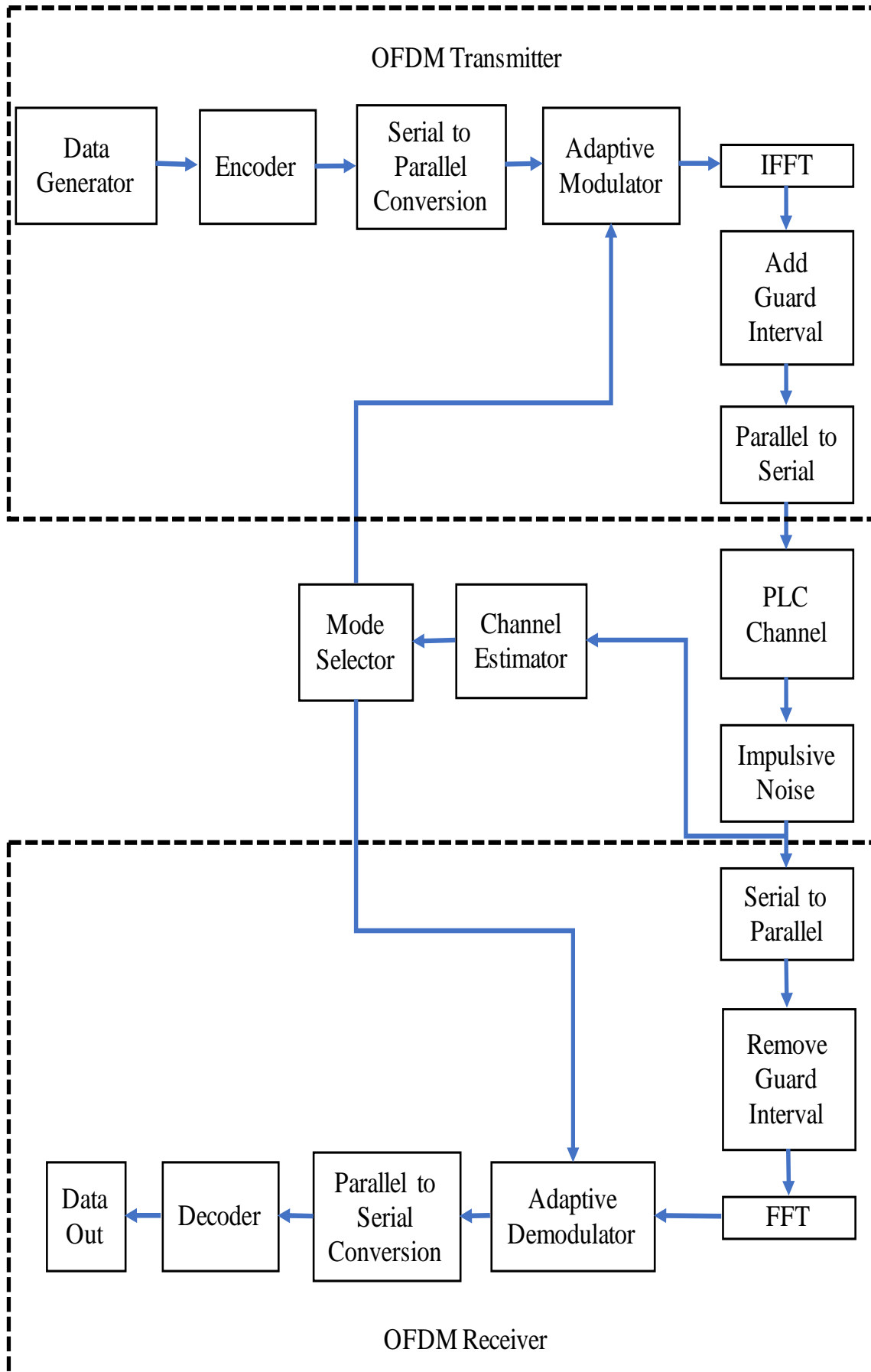


Figure 3.1. OFDM-AMC system model

3.1. OFDM System Model

Frequency Division Multiplexing (FDM) is one of the division multiplexing data communication techniques which have been used since 1960. The first communication systems with OFDM were used for the military purposes [35].

The data losses due to multipath channel and impulsive noise can be reduced thanks to the communication system which is generated by using many parallel narrowband carriers, without using high-speed channel equalizer. Rather than sending the signal as a package, sending the signal through many narrowband subcarriers enables each sub-carrier to experience flat fading channel conditions instead of frequency-selective channel conditions such as the powerline channel conditions.

The communication systems which have classical FDM signaling technique need several numbers of sinusoidal signal generators and the coherent receivers. This makes the system very complex and expensive. Thanks to OFDM signaling technique, which is designed by using many orthogonal sub-carriers to each other, the communication system gains from both bandwidth of the total signal and complex system design. Fig. 3.2 stands for the comparison of FDM and OFDM signal within bandwidth efficiency:

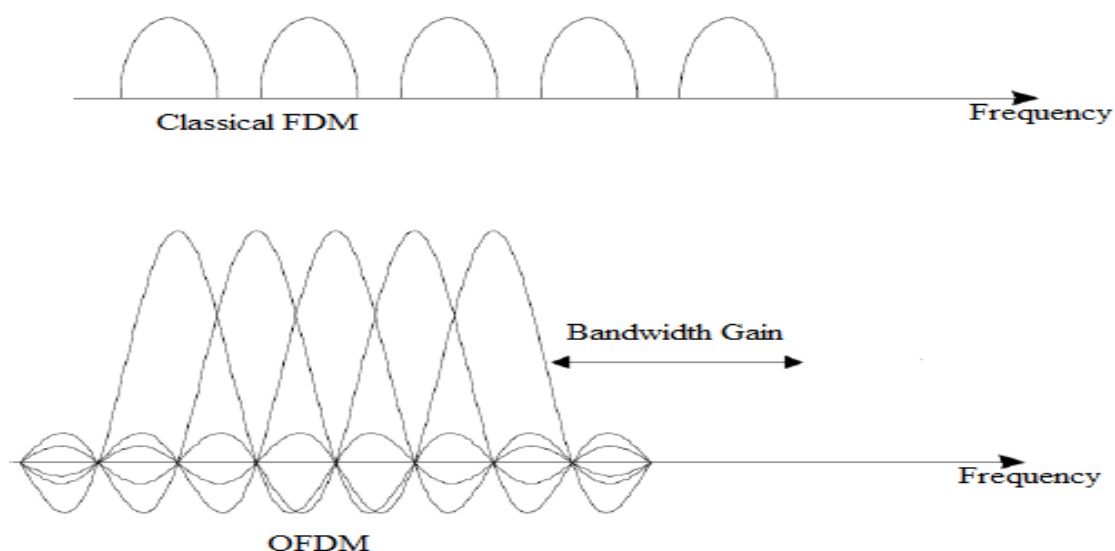


Figure 3.2. The comparison of the bandwidth gain between FDM and OFDM

The expression of orthogonality in OFDM modulation technique explains the mathematical relationship between the carrier sub-frequencies. There are a lot of carriers

in the standard FDM system. In order to provide orthogonalization in frequency space, guard band should be used between the carriers. This causes to decrease the efficiency of bandwidth. The side-bands of each carrier overlap in OFDM modulation technique; yet, the sub-carriers are independent of each other as can be seen in Fig.3.2. As it is illustrated in the figure, the bandwidth efficiency is increased with OFDM technique.

At the OFDM receiver, each sub-carrier of the signal is reduced to DC level. The reduced signal is gathered in sample period (τ), and herewith the sampling process is completed. The summation of the samples from other frequencies equal to zero as long as the other carriers satisfy the condition of integer number loops during the period of τ . If the gaps between other carriers are even to multiple of $1/\tau$ in frequency domain, the carriers can be expressing as linearly independent [8].

$$\int_a^b \psi_p(t) \cdot \psi_q^*(t) dt = 1, \quad p=q \quad (3.1)$$

$$\int_a^b \psi_p(t) \cdot \psi_q^*(t) dt = 0, \quad p \neq q \quad (3.2)$$

where ψ is a set of the signals formed by sub-carrier signals, and ψ_p stands for p th sub-carrier's waveform, $[a,b]$ interval is sampling period, and $(.)^*$ stands for the complex conjugate. If the condition of (3.2) is satisfied, this means that $\psi_p(t)$ and $\psi_q(t)$ are orthonormal signals.

The modulation system expression is based on equation (3.1) and (3.2). Mathematically, each carrier is expressed as a complex wave like in the following equation:

$$S(t) = A(t) \cdot \exp(j\omega t + \phi(t)), \quad (3.3)$$

where $A(t)$ and $\phi(t)$ stand for the amplitude and phase of the signal, respectively. The amplitude and the phase are constant during the sampling period. The real signal that is transmitted through the channel equals to the real part of $S(t)$.

As the OFDM system includes multiple sub-carriers, $S_s(t)$, the set of signals of OFDM can be expressed as follows:

$$S_s(t) = \frac{1}{N} \sum_{n=0}^{N-1} A_n(t) e^{j[\omega_n t + \phi_n(t)]}, \quad (3.4)$$

$$\omega_n = \omega_0 + n \Delta\omega, \quad (3.5)$$

$$\phi_n(t) = \phi(t), \quad (3.6)$$

$$A_n(t) = A(t). \quad (3.7)$$

If $S_s(t)$ is sampled with the frequency $1/T$, the discrete signal equation can be illustrated as follows:

$$S_s(kT) = \frac{1}{N} \sum_{n=0}^{N-1} A_n(t) e^{j[\omega_0 + n \Delta\omega]kT + \phi_n}. \quad (3.8)$$

Thus, the period of data sampling, τ , equals to $N.T$; and data can be notched up by using N number of sample. If the equation (3.8) is simplified, under the conditions of $\omega_0=0$ and $\phi_n=0$, the equation can be rearranged as follows:

$$S_s(kT) = \frac{1}{N} \sum_{n=0}^{N-1} A_n(t) e^{j[n \Delta\omega]kT}. \quad (3.9)$$

In addition to these equations, the processes of FFT and IFFT at OFDM transceiver which is shown in Fig. 3.1, can be expressed, respectively, as follows:

$$X_i = \sum_{n=0}^{N-1} x_i[n] e^{-j(2\pi/N)kn}, \quad (3.10)$$

$$x_i[n] = \frac{1}{N} \sum_k X_i[k] e^{j(2\pi/N)kn}. \quad (3.11)$$

Inter-Carrier Interference (ICI) and Inter-Symbol Interference (ISI) occur quite often over multipath channels. The cyclic prefix (CP) is used in OFDM modulation based communication systems in order to prevent ICI and ISI. The following section explores the CP technique in OFDM.

3.1.1. Cyclic prefix

The environment like a multipath channel which has a destructive and constructive extension of delayed signals degrades the baseband signal. This problem can be eliminated by the extension of the symbol with the cyclic prefix in OFDM [14]. Additionally, the CP provides the guard bands in FDM as shown in Fig. 3.3.

The CP can be achieved by copying the last length of sample of the symbol which is L , into the front of the OFDM symbol [6]. To limit the ISI; the length of the CP, L , should be equal to or longer than the delay spread of the multipath channel, in the frequency domain [6, 14]. Therefore, all the sub-carriers can be received independently at the receiver.

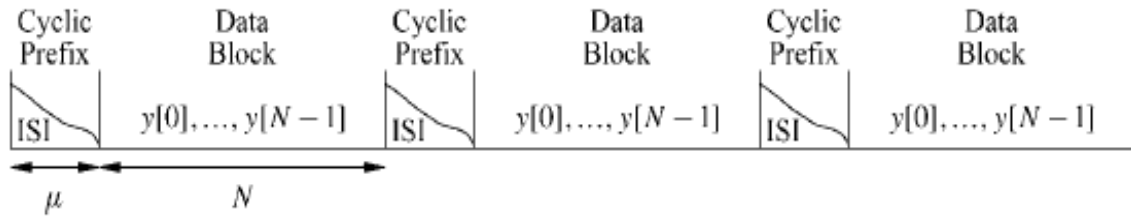


Figure 3.3. ISI between data blocks in channel output [14]

Assume that $Y[0]$ is an OFDM symbol with the length of N .

$$Y[0] = y[0], \dots, y[N-1]. \quad (3.12)$$

When the CP is added to the OFDM symbol the new OFDM symbol becomes as follows:

$$Y = y[N-L+1], y[N-L+2], \dots, y[0], \dots, y[N-1]. \quad (3.13)$$

The OFDM symbol passes through the process of Parallel to Serial Conversion after the CP addition.

3.1.2. Quadrature amplitude modulation/OFDM

For M-QAM, the information bits are encoded in both the amplitude and phase of the transmitted signal [14]. The bandwidth efficiency of Pulse-Amplitude Modulation-Single-Sideband (PAM/SSB) can also be acquired by impressing, at the same time, the two

separate k-bit symbols from the information sequence $[a_n]$ on two quadrature carriers $\cos(2\pi f_c t)$ and $\sin(2\pi f_c t)$ which is called Quadrature PAM or Quadrature Amplitude Modulation (QAM) with signal waveforms as follows:

$$\begin{aligned} S_m(t) &= \text{Re}\{(A_{mc} + jA_{ms}) g(t) e^{j2\pi f_c t}\}, \quad m=0, 1, \dots, M \\ & \quad 0 \leq t \leq T \\ &= A_{mc} g(t) \cos(2\pi f_c t) - A_{ms} g(t) \sin(2\pi f_c t), \end{aligned} \quad (3.14)$$

where A_{mc} and A_{ms} are the information-bearing amplitude of the quadrature carriers, and $g(t)$ is the signal pulse.

In other words, the signal waveform of QAM may be expressed as follows:

$$\begin{aligned} S_m(t) &= \text{Re}\{V_m e^{j\theta_m} g(t) e^{j2\pi f_c t}\}, \\ &= V_m g(t) \cos(2\pi f_c t + \theta_m), \end{aligned} \quad (3.15)$$

$$V_m = \sqrt{A_{mc}^2 + A_{ms}^2}, \quad (3.16)$$

$$\theta_m = \tan^{-1}\left(\frac{A_{ms}}{A_{mc}}\right), \quad (3.17)$$

As can be seen from the aforementioned expressions, the signal waveform of QAM is combination of amplitude and phase modulations.

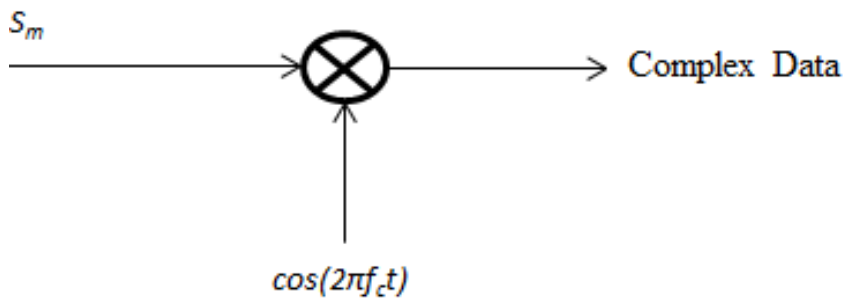


Figure 3.4. QAM modulator structure

We may choose any combination of M_1 -level PAM and M_2 -level PSK to set up $M = M_1 M_2$ associated PAM-PSK signal constellation. If $M_1 = 2^n$ and $M_2 = 2^m$, the combined PAM-PSK signal constellation results in simultaneous transmission of “ $m+n = \log_2 M_1 M_2$ ” binary digits at a symbol rate of $R / (m+n)$.

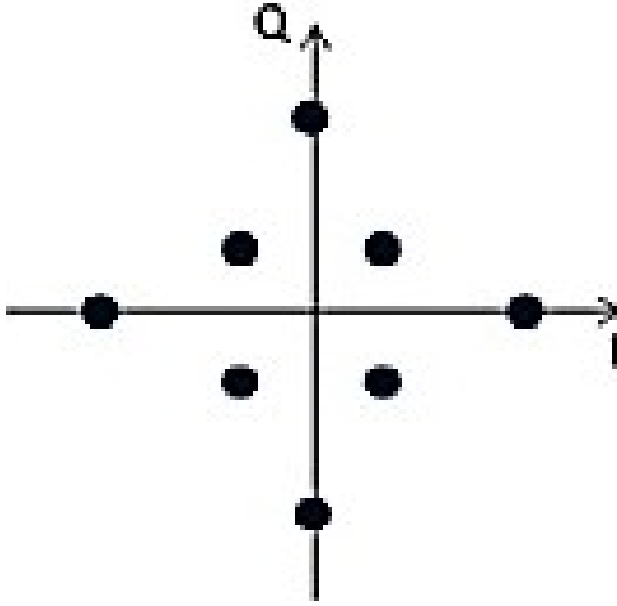


Figure 3.5. M=8 PAM-PSK signal space diagram [19]

The waveform of QAM signals can be represented as a linear combination of the two orthonormal signal waveforms, $f_1(t)$ and $f_2(t)$.

$$S_m(t) = S_{m1}f_1(t) + S_{m2}f_2(t), \quad (3.18)$$

$$f_1(t) = \sqrt{2/\varepsilon_g} g(t) \cos(2\pi f_c t), \quad (3.19)$$

$$f_2(t) = -\sqrt{2/\varepsilon_g} g(t) \sin(2\pi f_c t), \quad (3.20)$$

$$\begin{aligned} \underline{S}_m &= [S_{m1} \quad S_{m2}], \\ &= [A_{mc} \sqrt{2/\varepsilon_g} \quad A_{ms} \sqrt{2/\varepsilon_g}], \end{aligned} \quad (3.21)$$

where ε_g is the energy of the signal pulse $g(t)$. Euclidean distance between any pair of the signal vectors is:

$$\begin{aligned} d_{nm}^{(e)} &= \|\underline{S}_m - \underline{S}_n\|, \\ &= \sqrt{2/\varepsilon_g [(A_{mc} - A_{nc})^2 + (A_{ms} - A_{ns})^2]} \end{aligned} \quad (3.22)$$

In the special case of:

$$A_{mc}, A_{ms} = (2m-1-M)d, \quad m=1, \dots, M \quad (3.23)$$

The signal space diagram is rectangular with minimum distance:

$$d_{nm}^{(e)} = d \sqrt{2/\epsilon_g} \quad (3.24)$$

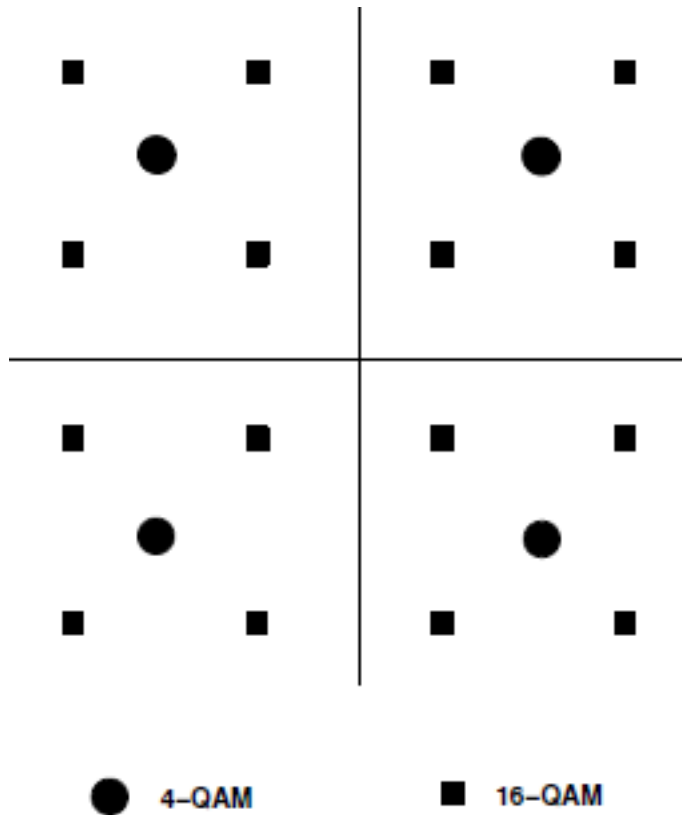


Figure 3.6. 4-QAM and 16-QAM constellations [14]

The constellation of 4-QAM and 16-QAM is shown in the Fig. 3.6. Each point in the constellation stands for a bit number. The data rate of the communication system can be increased by choosing the higher order schemes of QAM.

In this study, we use 4-QAM, 16-QAM, and 64-QAM schemes with two different coding rates of 1/2 and 3/4.

3.2. Link Adaptation (Adaptive Modulation and Coding)

Any data rate may be adaptively varied by the channel variation [6]. Adaptive modulation and coding (AMC) technique boosts the spectral efficiency over time-varying channels [14]. The AMC system requires certain channel state information (CSI) at the transmitter.

The CSI is estimated at the receiver and is fed back to the transmitter. Thus, the modulation scheme and coding rate can be adapted and set for the next OFDM symbol. At

the same time, the receiver should be fed back from the channel estimator to adapt the next symbol.

The communication systems which have fixed modulation scheme and coding rate require to be designed in the case of the worst-case scenario in order to operate when the quality of the channel is very poor. This indicates that AMC technique performs better at time-variant channel conditions such as powerline channel.

The average throughput can be increased; and both the required power for transmitter and the probability of bit-error can be reduced by controlling modulation scheme and coding rate according to the channel conditions. The basic AMC system model is given in the Fig. 3.7.

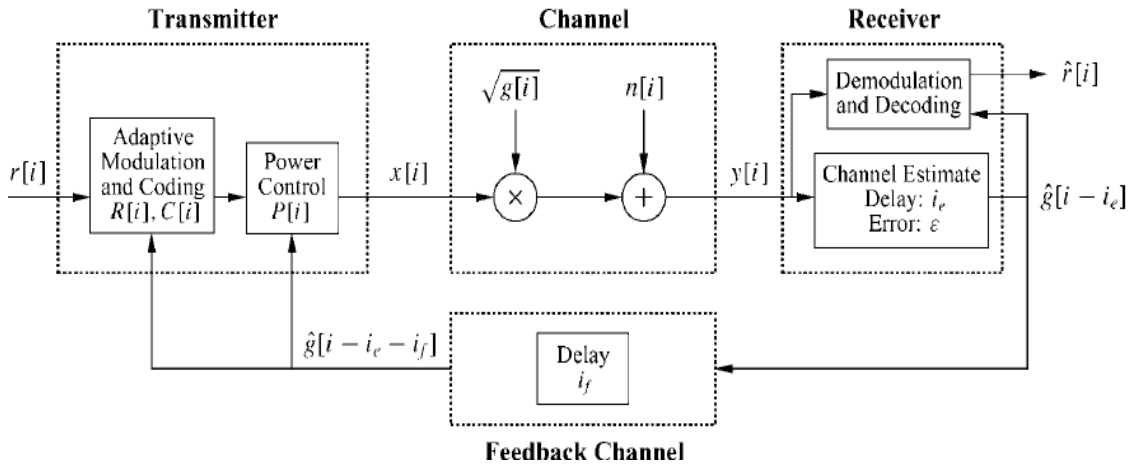


Figure 3.7. AMC system model

The approximate bit and symbol error probability for QPSK and rectangular MQAM is calculated, respectively, as follows:

$$P_b \approx Q(\sqrt{2\gamma_b}), \quad (3.25)$$

$$P_s \approx 2Q(\sqrt{\gamma_s}), \quad (3.26)$$

$$P_b \approx \frac{4}{\log_2 M} Q\left(\sqrt{\frac{3\gamma_b \log_2 M}{M-1}}\right), \quad (3.27)$$

$$P_s \approx 4Q\left(\sqrt{\frac{3\gamma_b \log_2 M}{M-1}}\right), \quad (3.28)$$

where M stands for modulation order, γ_b stands for the energy of bit, and γ_s stands for energy of the symbol.

In this study, we use minimum-mean-square-error estimator (MMSE) to estimate channel state information at the receiver. Once the MMSE estimator evaluates the instantaneous SNR in the channel, the mode selector gives feedback to the transmitter in order to adapt constellation scheme and coding rate. The coding rate and modulation scheme are adjusted according to SNR thresholds which are acquired from the performance of each scheme in the PLC channel possessing target BER of 0.001. In the flow of this study, the SNR thresholds will be given in the simulation section. The channel estimation which is necessary at the receiver side is explored in the following section.

3.2.1. Channel estimation

The signal which is transmitted over a channel is generally exposed to distortions by the channel conditions. In order to repair the damaged bits, the effect of the channel should be estimated and atoned at the receiver side [34]. By using the known symbols at the transmitter and the receiver, the channel may be estimated. The interpolation of the pilot symbol makes the estimation of the channel response of the subcarriers between pilot tones possible [6].

There are various types of channel estimation in the literature such as Least Square (LS) estimation [7], Minimum-Mean-Square-Error (MMSE) estimation [34], maximum likelihood (ML) estimator [33], and the parametric channel modeling-based (PCMB) [36] estimator. In this study, we utilize one of the training symbol-based estimators which is MMSE estimator that is explained in the following section.

Minimum-mean-square-error estimator

Assume that H is the channel vector that is given as $H = [H[0], H[1], \dots, H[N-1]]^T$, and \hat{H} is the estimation of the channel H , and Z denotes the noise vector which is given as $Z = [Z[0], Z[1], \dots, Z[N-1]]^T$.

The minimum-mean-square-error of the channel estimate \hat{H} is given as follows:

$$J(\hat{\mathbf{H}}) = E\{\|\mathbf{e}\|^2\} = E\{\|\mathbf{H} - \hat{\mathbf{H}}\|^2\}$$

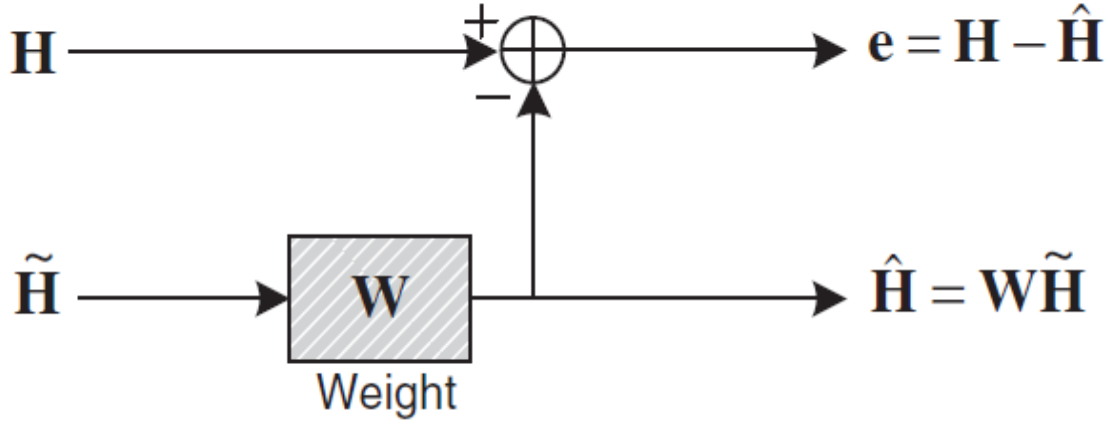


Figure 3.8. MMSE channel estimation [6]

$$J(\hat{H}) = E\{\|e\|^2\} = E\{\|H - \hat{H}\|^2\}. \quad (3.29)$$

The orthogonality basis defines that the estimation error vector which $e = H - \hat{H}$ is orthogonal to \hat{H} . Thus:

$$\begin{aligned} E\{e \hat{H}^H\} &= E\{(H - \hat{H}) \hat{H}^H\} \\ &= E\{(H - W\hat{H}) \hat{H}^H\} \\ &= E\{(H - W\hat{H}) \hat{H}^H\} \\ &= E\{H\hat{H}^H\} - WE\{\hat{H}\hat{H}^H\} \\ &= R_{H\hat{H}} - WR_{\hat{H}\hat{H}} = 0 \end{aligned} \quad (3.30)$$

where R is the $N \times N$ cross-correlation matrix of the A and B matrices, and \hat{H} is the least-square channel estimate can be defined as:

$$\hat{H} = X^{-1}Y = H + X^{-1}Z. \quad (3.31)$$

Rearranging the equation in (3.30) for yields of W can be denoted as follows:

$$W = R_{H\hat{H}} R_{\hat{H}\hat{H}}^{-1}, \quad (3.32)$$

where $R_{\hat{H}\hat{H}}$ represents an auto-correlation matrix of \hat{H} is shown as:

$$\begin{aligned}
R_{H\hat{H}} &= E\{\hat{H}\hat{H}^H\} \\
&= E\{X^{-1}Y(X^{-1}Y)^H\} \\
&= E\{(H+X^{-1}Z)(H+X^{-1}Z)^H\} \\
&= E\{H\hat{H}^H + X^{-1}ZH^H + HZ^H(X^{-1})^H + X^{-1}ZZ^H(X^{-1})^H\} \\
&= E\{H\hat{H}^H\} + E\{X^{-1}ZZ^H(X^{-1})^H\} \\
&= E\{HH^H\} + \frac{\sigma_z^2}{\sigma_x^2} I.
\end{aligned} \tag{3.33}$$

where $R_{H\hat{H}}$ matrix stands for the cross-correlation between the temporary channel estimate and true channel vectors in the frequency space. Finally, by using the equation in (3.33), the minimum-mean-square-error estimation can be denoted as:

$$\begin{aligned}
\hat{H} &= W\hat{H} = R_{H\hat{H}}^{-1} R_{\hat{H}\hat{H}} \hat{H} \\
&= R_{H\hat{H}} (R_{HH} + \frac{\sigma_z^2}{\sigma_x^2})^{-1} \hat{H}.
\end{aligned} \tag{3.34}$$

3.2.2. Turbo coding

In 1949, the study [30] which is including the mathematical basis for the noisy communication channel is published in 1949 by Claude Shannon. The maximum channel capacity, namely, the Shannon limit, is determined in this study by stating that a channel coding technique should exist in the communication system to reach Shannon limit. In the following years, there have been done various types of research about channel coding to reach towards to Shannon limit. Yet, these studies demanded large block lengths which led to high cost, and complexity. However, these studies showed that there is gain about BER performance at higher signal-to-noise ratio.

In 1993, Berrou et al. proposed their study [4] which offers a new approach to convolutional codes named turbo-codes. The study shows that it is possible to reach 0.7 dB of Shannon limit by using turbo coding technique.

The turbo codes are the kind of the forward error correction (FEC) codes, which include the coder and the decoder blocks.

Coding

Turbo codes consist of input and output codes which are merged through an Interleaver. Turbo coder consists of two Recursive Systematic Convolutional Encoders (RSC) parallel to each other and the interleaver between two RSC encoders as shown in the Fig. 3.9.

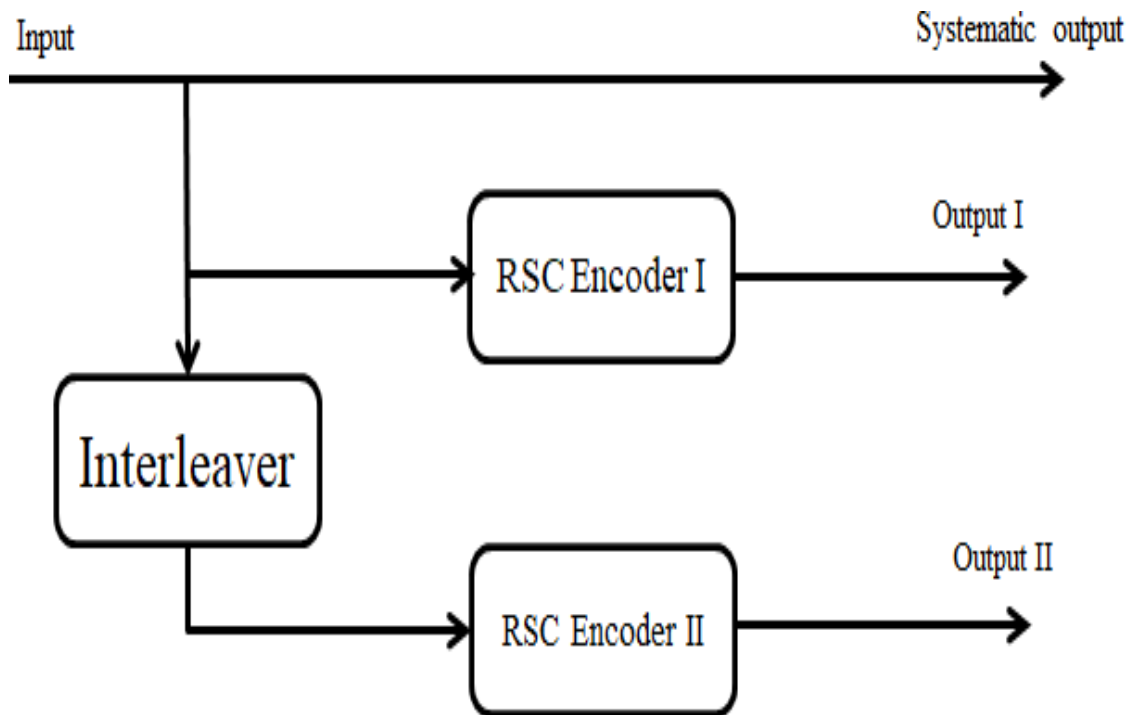


Figure 3.9. A turbo coder with 1/3 coding rate

As can be seen from the Fig. 3.9, the input data is directly connected to the RSC Encoder I, and RSC Encoder II following the interleaving process. The interleaver modifies the input data sequence under specific principles. The data from interleaver structure is necessary for the decoding process at the OFDM receiver [14].

Structure of the recursive systematic convolutional encoder

Turbo codes are components of the concatenated codes which include the interleavers, and the recursive systematic convolutional encoders. The RSC encoder is given in Fig. 3.10 derived from a convolutional coder which is given in Fig. 3.11. The code is generated by the generator matrix $G[111;101]$. As can be seen in Fig. 3.10/3.11, the RSC coder is established by collecting feedback from the output c_0 to input. Thus, c_0 indicates the systematic data sequence while c_2 indicates the coded data sequence [23].

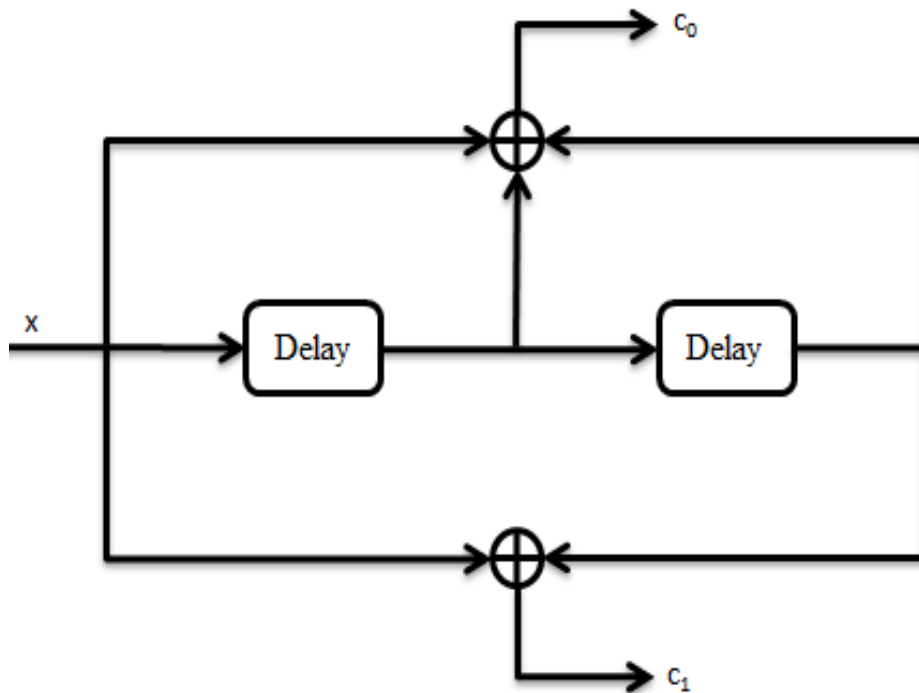


Figure 3.10. Convolutional coder, $G[111;101]$

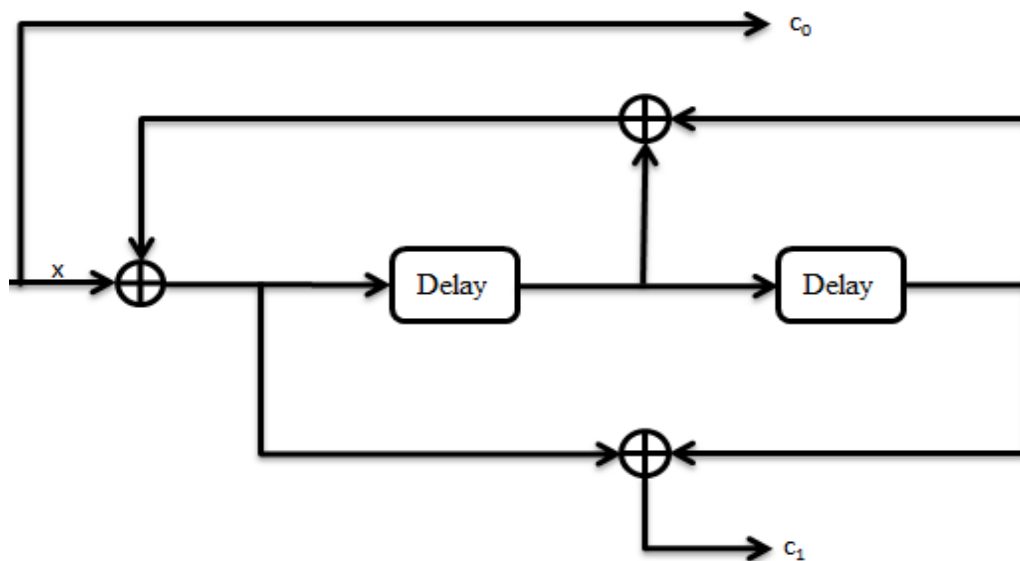


Figure 3.11. Recursive systematic convolutional coder, $G[111;101]$

The interleaver

The primary goal of the interleaver is fundamentally to reform the data. The interleaver revises the data at its input which is already loaded according to the noise; and gives a different type of data as its output. The opposite operation of this process is used for the separation of the original data from the received data. The interleaving process is a handful technique which increases the capacity of the coding process. This process is used just

before the second RSC encoder which is shown in Fig. 3.9. Its main aim is to establish the large block codes, and to approach to Shannon's limit, from the small memory convolutional codes. The interleaver process designs the scrambled data sequence to RSC encoder II. This condition leads to decorrelation between the two decoders, and thus, the interleaving process allows application of the BCJR algorithm [2] which depends on the exchange of the uncorrelated data between the two decoder blocks. In this way, some parts of incorrect data can be verified at the first decoder, and the rest of the data can be verified at the second decoder. The block interleaver, is given in Fig. 3.12, with n number of columns and d number of rows.

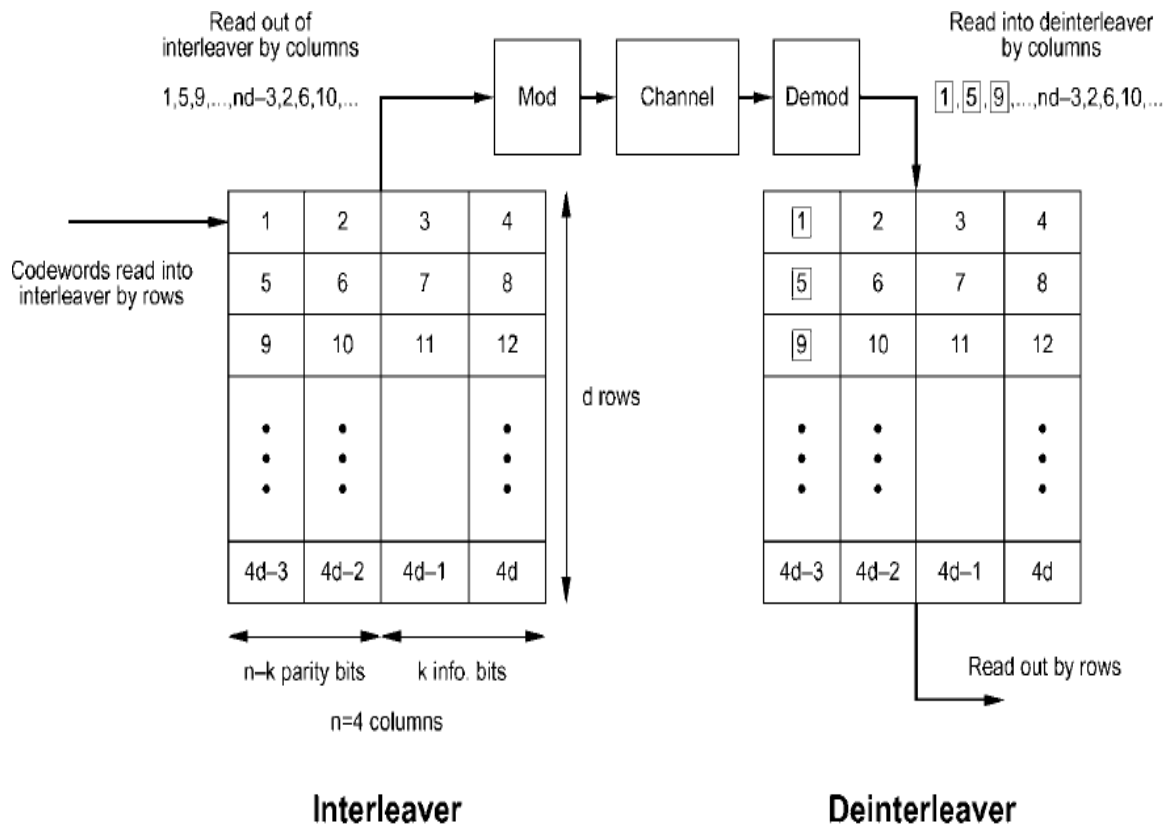


Figure 3.12. The interleaver and the deinterleaver operations [14]

Trellis diagram

The trellis diagram explains the behavior of the turbo encoder from the first data stream to the end, and also it is indispensable for code decoding. The trellis is finalized by adding $m = K - 1$ bit queue data to the end of the input data sequence, in which K stands for the number of the rows in the generator matrix G . These added bits lead to switch the encoder to all zero state. This process is called as trellis termination.

3.2.3. Turbo decoder

The turbo decoder, given in Fig. 3.13, includes the double decoders to improve the estimation of the original data stream. The decoders' working principle depends on the Maximum Posteriori Probability (MAP) algorithm which is also known as BCJR algorithm [2]. The operation processes according to the soft decision information which is fed-back from one decoder to other. The remaining data is acquired from the soft decision operation at the decoder 1, and called temporary information, L_e . This information goes through the decoder 2, following the deinterleaving process. The decoder 2 evaluates the data and tries to compose the best estimation. After this process; the data, at the output of the decoder 2, is transmitted to the decoder 1 via the interleaving operation. Following this step, the decoder 1 starts to work for the estimation of the data. This loop operation continues until the soft decision sets to a constant value.

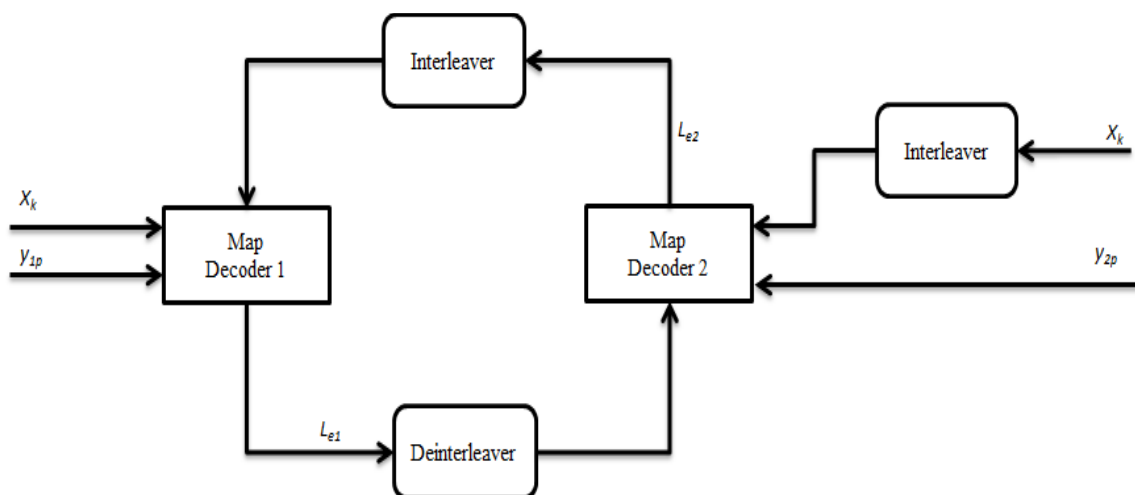


Figure 3.13. Turbo decoder

The y_{1p} , y_{2p} , and x_k stand for systematic bits and a parity bit, respectively; the L_{e1} and L_{e2} stand for the information between decoders at turbo decoder diagram which is given in Fig. 3.13.

Maximum a posteriori probability (MAP) algorithm / BCJR algorithm

In 1993, Bahl, Cocke, Jelinek, and Raviv published their study [2] is named as BCJR algorithm which is a decoder for the turbo codes. This algorithm is crucial for the modern iterative decoding and error correction codes systems such as the low-density parity-check

codes. The BCJR algorithm is trellis-based decoding algorithm which decodes every information bit in accordance with MAP criteria in the convolutional code.

The transmitted information data is $z_k = \{x_k, y_{ik}\}$, $i=1,2$, where x_k stands for systematic code, and y_{ik} stands for parity check codes at the output of the RSC encoder I and II.

The received code components are $z'_k = \{x'_k, y'_{ik}\}$, $i=1,2$, and $z' = z'_{1,N} = \{z'_1, z'_2, \dots, z'_N\}$ where N is the length of the data.

The temporary information from the decoder i to the decoder j is $L_{ei,j}$ where $i, j = 1,2$.

The soft decision of the MAP is illustrated as:

$$L_{map}(x_k) = \log\left(\frac{P_r(x_k = +1I z')}{P_r(x_k = -1I z')}\right). \quad (3.35)$$

The next equation is acquired by applying to Bayes theorem to the numerator and denominator of the L_{map} is:

$$\frac{P_r(x_k = +1I z')}{P_r(x_k = -1I z')} = \frac{\sum_{(s', s) \in S^+} P_r(s_{k-1} = s', s_k = s, z')}{\sum_{(s', s) \in S^-} P_r(s_{k-1} = s', s_k = s, z')}. \quad (3.36)$$

$$P_r(s_{k-1} = s', s_k = s, z'_{1,N}) = P_r(s_{k-1} = s', z'_{1,k-1}), \quad (3.37)$$

$$P_r(s_{k-1} = s', z'_{1,k} | s_{k-1} = s') \cdot P_r(z'_{k+1,N} | s_k = s) = \alpha_{k-1}(s') \cdot \gamma_k(s', s) \cdot \beta_k(s), \quad (3.38)$$

$\alpha_k(s')$ shows that the common probability of the status value of the condition k and the observed output values up to that moment. This function can be rearranged by using $\gamma_k(s', s)$ as in the following equation:

$$\begin{aligned} \alpha_k(s) &= \sum_{s'} P_r(s_{k-1} = s', z'_{1,k-1}) P_r(s_k = s, z'_k | s_{k-1} = s') \\ &= \sum_{s'} \alpha_{k-1}(s') \gamma_k(s', s), \end{aligned} \quad (3.39)$$

After the normalization process $\alpha_k(s)$ can be expressed as follows:

$$\alpha_k(s) = \frac{\sum_{s'} \alpha_{k-1}(s') \gamma_k(s', s)}{\sum_s \sum_{s'} \alpha_{k-1}(s') \gamma_k(s', s)} \quad (3.40)$$

$\beta_k(s')$, is the conditional probability of the observable output values after the known conditions at the moment of k . This function can be rearranged by using $\gamma_k(s', s)$ as in the equation:

$$\begin{aligned} (z'_{k+1,N} I s_k = s) &= \sum_s P_r(s_{k+1} = s, z'_{k+1} I s_k = s') \cdot P_r(z'_{k+2} I s_k = s') \\ &= \sum_{s'} \gamma_{k+1}(s', s) \beta_{k+1}(s) \end{aligned} \quad (3.41)$$

After the normalization process the β function can be expressed as follows:

$$\beta_k(s') = \frac{\sum_{s'} \beta_{k+1}(s) \gamma_{k+1}(s', s)}{\sum_s \sum_{s'} \beta_{k+1}(s) \gamma_{k+1}(s', s)} \quad (3.42)$$

Finally, $\gamma_k(s', s)$ is the condition of z'_k 's bit, which is previous known value, at the k moment; and the probability of the output value at that moment. Eq. 3.43 shows this function as follows:

$$\gamma_k(s', s) = \exp\left(\frac{1}{2}(x_k L_a(x_k) + x_k L_c x'_k + p_k L_k p'_k)\right) \quad (3.43)$$

where L_a stands for a priori information that comes from the decoder block. In the context of the mentioned mathematical equations, BCJR is feasible to decode the convolutional and the block codes.

4. MULTIPLE-INPUT MULTIPLE-OUTPUT POWERLINE COMMUNICATIONS

The main aim of the communication systems is to possess high spectral efficiency, high-capacity, high-speed, and high reliability. The multiple-input multiple-output (MIMO) systems are basically used to achieve the Shannon's limit. The first study is published by Winters [20], Foschini [13], Foschini and Gans [12], and Telatar [9]. In addition to gain of spectral efficiency, using MIMO antenna technique decreases ISI [14].

There are four types of MIMO systems such as single-input single-output (SISO), single-input multiple-output (SIMO), multiple-input single-output (MISO), and multiple-input multiple-output (MIMO). The input of the MIMO channel represents the starting point of the powerline and the output of the MIMO channel shows the OFDM receiver. The aforementioned multi-antenna systems can be examined according to their placement in the system. Multiple antennas are installed at the transmitter of the OFDM system feasible for beamforming [27]. Multiple antennas at the transmitter or receiver of the communication systems are used for achieving various diversity schemes including space-time and space-frequency coding [26]. Multiple antennas at both the receiver and the transmitter of the systems are used for spatial multiplexing [5]. There are also adaptive methods such as the combination of diversity and spatial multiplexing [17], and the combination of beamforming and spatial multiplexing [31]. In this study, we utilize the spatial multiplexing in the communications system.

[29] is the first study on broadband MIMO-PLC. The highly distortive communication environments such as the multipath fading like MIMO powerline channel causes the channel to be frequency selective fading [37]. OFDM technique may transform the frequency selective fading MIMO channel into the flat fading channel. Thus, the combination of adaptive modulation coding, OFDM, and MIMO is promising for broadband communications in the powerline.

The powerline is a good candidate for the communication in broadband by using MIMO technique due to available multiple cables in the system. The system has three wires such as Phase (P), Neutral (N), and Protective Earth (PE), so SISO, 2x2, and 3x3 MIMO spatial multiplexing is applicable for the PLC communication. In the form of a spatial

multiplexing, OFDM symbols are transmitted with different antennas simultaneously and with the same frequency. Thus, the channel capacity is increased by this technique. The next section expresses the MIMO channel and shows the measurements over MIMO channel.

4.1. MIMO-PLC Channel Model

There are three wires available in the powerline which are phase (P), neutral (N), and protective earth (PE). The traditional PLC system employs the single-input single-output (SISO) channel as it uses only one port which is PN port to both transmit and receive the data. If the wire PE is installed, all the wires may form 3 ports which are P-N, N-PE, and P-PE. Thus, 3x3 MIMO communication system can be acquired as shown in the Fig. 4.1.

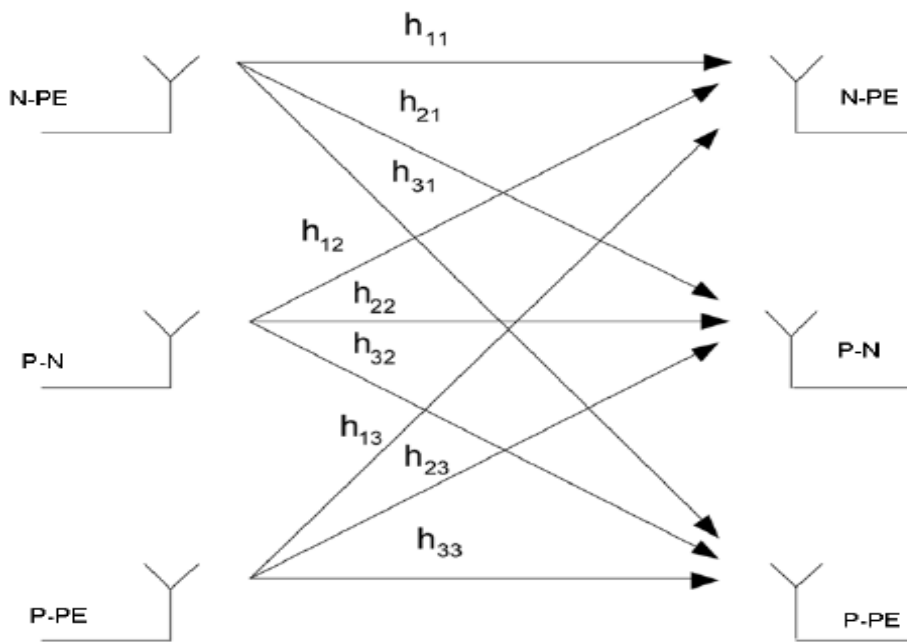


Figure 4.1. MIMO-PLC channel model

The MIMO channel matrix $H(f)$ can be expressed as follows:

$$H(f) = \begin{bmatrix} h_{11}(f) & h_{12}(f) & h_{13}(f) \\ h_{21}(f) & h_{22}(f) & h_{23}(f) \\ h_{31}(f) & h_{32}(f) & h_{33}(f) \end{bmatrix}, \quad (4.1)$$

where N is the number of receiver antennas (ports), M is the number of transmitter antennas (ports), $h_{NM}(f)$ stands for the channel transfer coefficient, at the frequency f ,

from m^{th} transmitter antenna to n^{th} receiver antenna. If $m=n$, then the channels should be called as co-channels, and if $m \neq n$, then the channels should be called as cross-channels [28].

The multipath fading PLC channel (SISO mode) model is published by Zimmermann in [40] expresses the transfer function as follows:

$$H(f) = \sum_i^N g_i \cdot e^{-(a_0+a_1 f^k) d_i} \cdot e^{-j2\pi f (d_i/v_p)}, \quad (4.2)$$

where $H(f)$ is the frequency response of the multipath channel, d_i stands for the length of path, g_i is the weighting factor, k is the attenuation factor, a_0 and a_1 are attenuation parameters.

In 2009, Tonello and Versolatto published the statistical extension of Zimmermann's model in [32]. The PLC channel's expected path-loss (PL) is expressed by Tonello is as follows:

$$PL_{a_0, a_1, K}(f) = A^2 \frac{\Lambda}{3} \frac{1 - e^{-2L_{max}(a_0 a_1 f^K)}}{(2a_0 + 2a_1 f^K)(1 - e^{-\Lambda L_{max}})}, \quad (4.3)$$

where A, K, a_0 , and a_1 stand for attenuation factors, Λ has a characteristic of Poisson distribution, and L_{max} shows the maximum length of signal paths. The required parameters are given for the statistical model of PL [3] in Table 4.1.

To extend single-input single-output PLC channel model into the multiple-input multiple-output PLC channel matrix, the Pearson correlation coefficient, which is published in [28] and expressed with ρ , should be computed on the normalized channel transfer function (CTF). The normalized CTF is given as Eq. 4.4:

$$\tilde{h}_{S_n D_m}(f) = \frac{h_{S_n D_m}(f)}{\sqrt{PL_{S_n D_m}(f)}}, \quad (4.4)$$

Table 4.1. The statistical CTF parameters

Path Loss Parameter	Model	Parameters
$A_{\text{dB}S_1,D_1}$	$\mathcal{N}(\mu_A, \sigma_A)$	$\mu_A = -50.1$ dB $\sigma_A = 15.6$ dB
$A_{\text{dB}S_m,D_m}$ ($m \in [1-3]$)	$A_{\text{dB}S_m,D_m} = A_{\text{dB}S_1,D_1} + \mathcal{N}(0, \sigma_{S_m,D_m})$	$[\sigma_{S_m,D_m}] = \begin{bmatrix} 0 & 5.1 & 3.8 \\ 2.9 & 5.7 & 5.2 \\ 6.6 & 7.8 & 6.9 \\ 4.6 & 5.9 & 5.1 \end{bmatrix}$ dB
$A_{\text{dB}S_4,D_4}$	$A_{\text{dB}S_4,D_4} = 0.5 \times A_{\text{dB}S_1,D_1} - 30 + \mathcal{N}(0, \sigma_{S_4,D_4})$	
a_0	$\mathcal{E}_{\text{sig}}(\mu_{a0}, \delta_{a0})$	$\mu_{a0} = 1.04 \times 10^{-2}$ $\delta_{a0} = -6.7 \times 10^{-3}$
a_1	Constant	$a_1 = 4 \times 10^{-10}$
K	$\mathcal{W}(\alpha_K, \beta_K)$	$\alpha_K = 5.7 \times 10^{-2}$ $\beta_K = 57.7$
L_{max}	Constant	$L_{\text{max}} = 800$ m
Λ	Constant	$\Lambda = 0.2$ m ⁻¹

Note: Parameters a_0 , a_1 and K are dimensionless.

where $h_{S_n D_m}(f)$ stands for the channel transfer function between the input antenna D_m and the output antenna S_n , and $PL_{S_n D_m}(f)$ denotes the own expected PL given in Equation (4.3).

$h_{S_n D_m}(f)$ is the complex correlation coefficient and channel transfer function $h_{S_i D_j}(f)$ in the matrix of MIMO can be calculated according to the following equation:

$$\rho_{S_n D_m, S_i D_j} = \frac{\langle \tilde{h}_{S_n D_m}(f) \tilde{h}_{S_i D_j}^*(f) \rangle - \langle \tilde{h}_{S_n D_m}(f) \rangle \langle \tilde{h}_{S_i D_j}^*(f) \rangle}{\sqrt{(\langle |\tilde{h}_{S_n D_m}(f)|^2 \rangle - |\langle \tilde{h}_{S_n D_m}(f) \rangle|^2) (\langle |\tilde{h}_{S_i D_j}(f)|^2 \rangle - |\langle \tilde{h}_{S_i D_j}(f) \rangle|^2)}}, \quad (4.5)$$

where $\langle \rangle$ shows the frequency domain average, and $*$ shows the operation of complex conjugate.

After the calculation of the correlation features of the MIMO matrix, the comprehensive MIMO-PLC channel can be expressed. The channel transfer function of the MIMO-PLC definition is as follows:

$$H(f) = A \sum_{p=1}^{N_p} g_p \cdot e^{-j\varphi_p} \cdot e^{-(a_0 + a_1 f^k) d_p} \cdot e^{-j2\pi f(d_p/v_p)}, \quad (4.6)$$

where A , K , a_0 , and a_1 stand for attenuation factor, d_p is the length of path, g_p is the weighting factor, and φ_p denotes additional phase is assigned to each path. According to the uniform distribution $-\Delta\varphi/2$ and $\Delta\varphi/2$, φ_p values are drawn randomly [28].

To maintain the adequate values of $\Delta\varphi$, the following values are recommended by the Monte Carlo simulations given in [3]:

In order to generate the channel D1-S2 from the channel D1-S1, and the channel D1-S3 from the channel D1-S1, adjust $\Delta\varphi$ to 2π .

For $m=1, \dots, 4$, in order to generate the channel D2-S m from D1-S m , and the channel D3-S m from the link D1-S m , adjust $\Delta\varphi$ to $4\pi/3$.

The example of the channel transfer function using the statistical model of MIMO-PLC is given in Fig. 4.2 from the study [3]. In order to provide clarity, the example includes only four channels from one Tx (D1 only) to four Rx antennas.

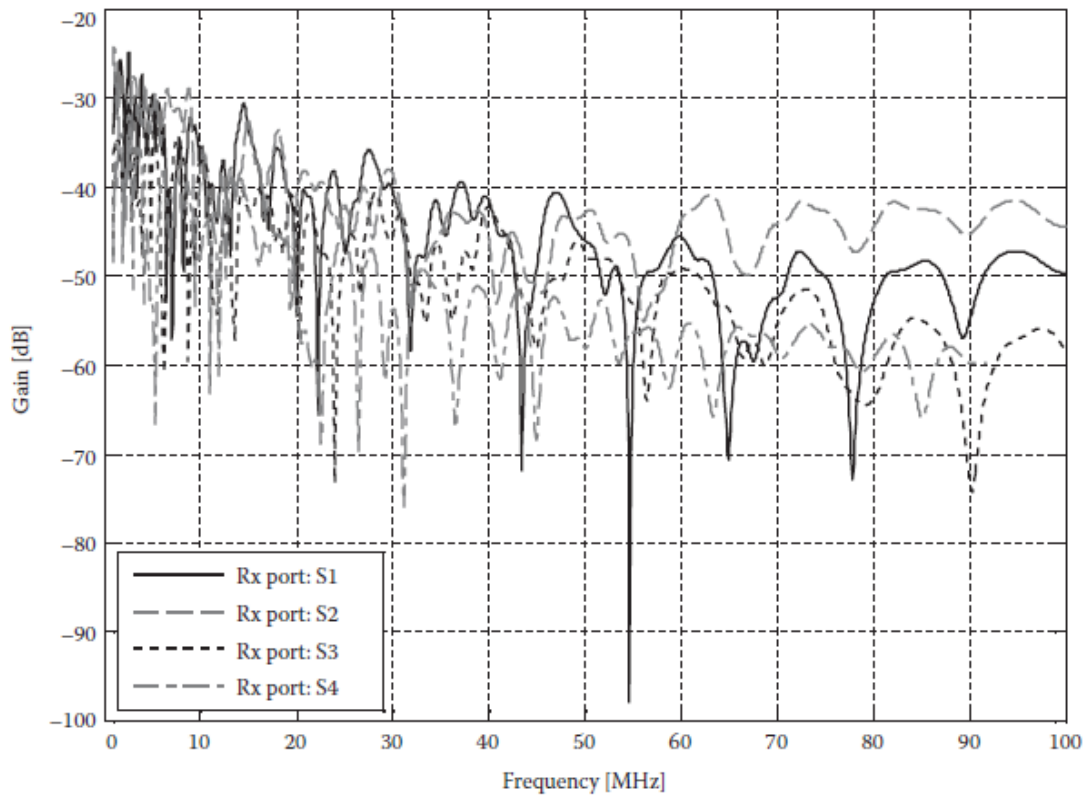


Figure 4.2. Example of MIMO-PLC channel transfer function based on the proposed statistical MIMO model (Tx: D1 only) [3]

5. SIMULATION RESULTS AND DISCUSSIONS

In this thesis, we investigate the Adaptive Modulation and Coding MIMO-OFDM spatial multiplexing in Broadband Powerline Communication. The bit-error-rate performances are compared according to different modulation schemes, coding rates, and the number of transmit and receive antennas. The powerline communication system is modelled by using MATLAB and SNR vs. BER graphics are acquired by running Monte Carlo simulations.

In order to compare BER performances of each system, M-QAM modulation scheme is utilized by using $M=4, 16, 64$, and as Forward Error Correction (FEC), the turbo coding with rates $\frac{1}{2}$ and $\frac{3}{4}$ are utilized. To achieve adaptive modulation and coding the required channel state information is acquired by using minimum-mean-square-error (MMSE) estimation method. As a channel model, we utilize one of the most popular channel models in broadband powerline communication channel which is Zimmermann's multipath channel model [40], and as a noise model in the channel the Middleton Class A noise model [41] is installed.

The adaptive modulation and coding technique is applied to both SISO channel, and MIMO channels. To achieve multiple-input multiple-output powerline communication system, 2x2 and 3x3 MIMO systems are utilized.

The spatial multiplexing technique is used for MIMO-PLC communication. The Zimmermann's channel transfer function is extended for the MIMO channel transfer function. SISO-PLC, 2x2, and 3x3 MIMO-PLC systems are compared according to their BER performance by using AMC technique.

The BER vs SNR graphic is given in Fig. 5.1 for SISO 4-path channel. According to the results, QPSK with $\frac{1}{2}$ and $\frac{3}{4}$ coding rate have better BER performances than 16-QAM and 64-QAM with $\frac{1}{2}$ and $\frac{3}{4}$ coding rate, under 4-path fading channel. In addition to this, each modulation scheme has better performance when $\frac{1}{2}$ coding rate compared to $\frac{3}{4}$ coding rate is used. Thus, one may assume that the lower modulation orders and coding rates are more suitable for better BER performance. Likewise, higher modulation orders and coding rates are more preferable to get higher throughput, which is a trade-off. The

modulation order and coding rate should be adjusted according to SNR thresholds are acquired from performance of the each scheme in the PLC channel possessing target BER of 0.001. The signal-to-noise ratio thresholds are given in Table 5.1.

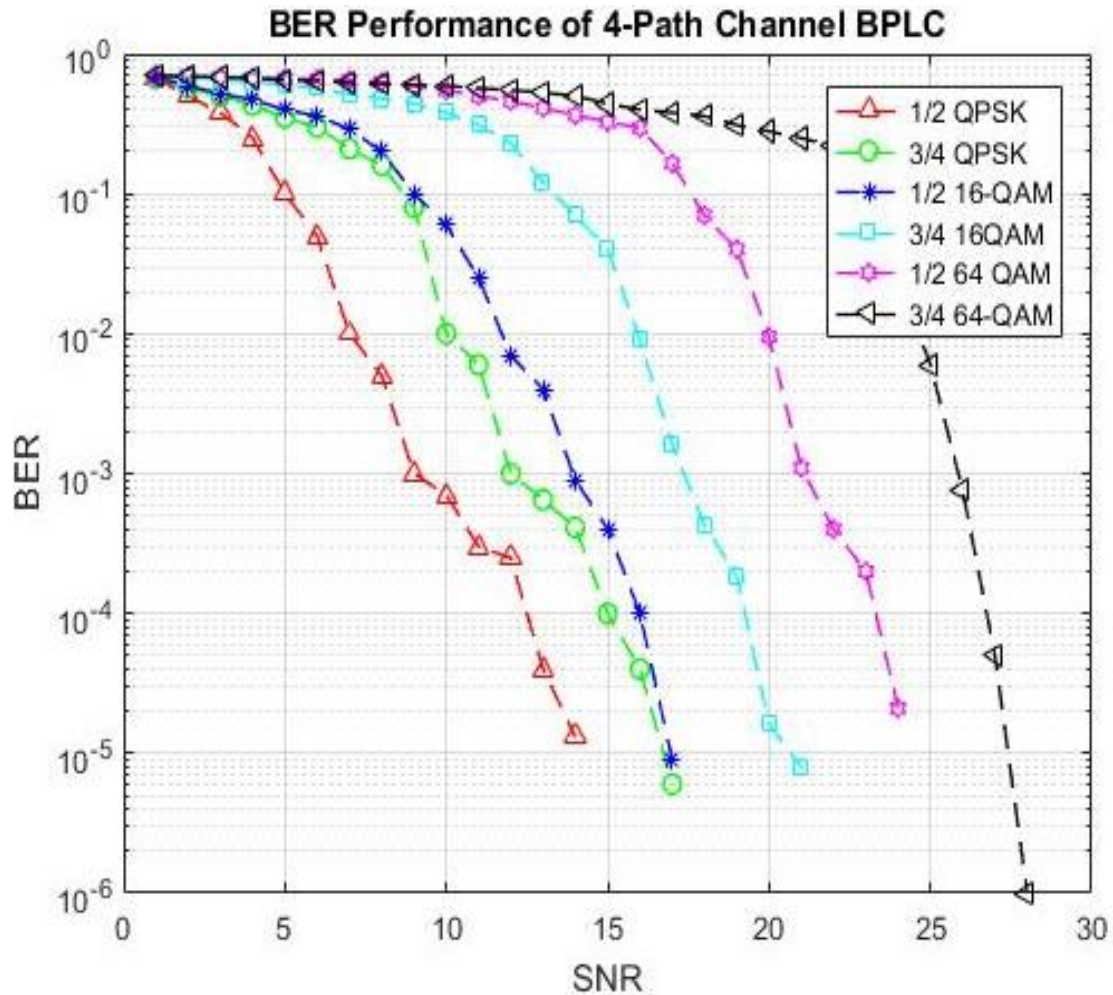


Figure 5.1. 4-path fading channel BER performance

Table 5.1. SNR thresholds modulation coding table

Modulation Order	Coding rate	SNR (dB)	
		4-path	15-path
QPSK	1/2	8,96	11,72
	3/4	11,88	14,8
16-QAM	1/2	13,94	17,38
	3/4	17,4	20,82
64-QAM	1/2	21,08	24,18
	3/4	25,86	27,56

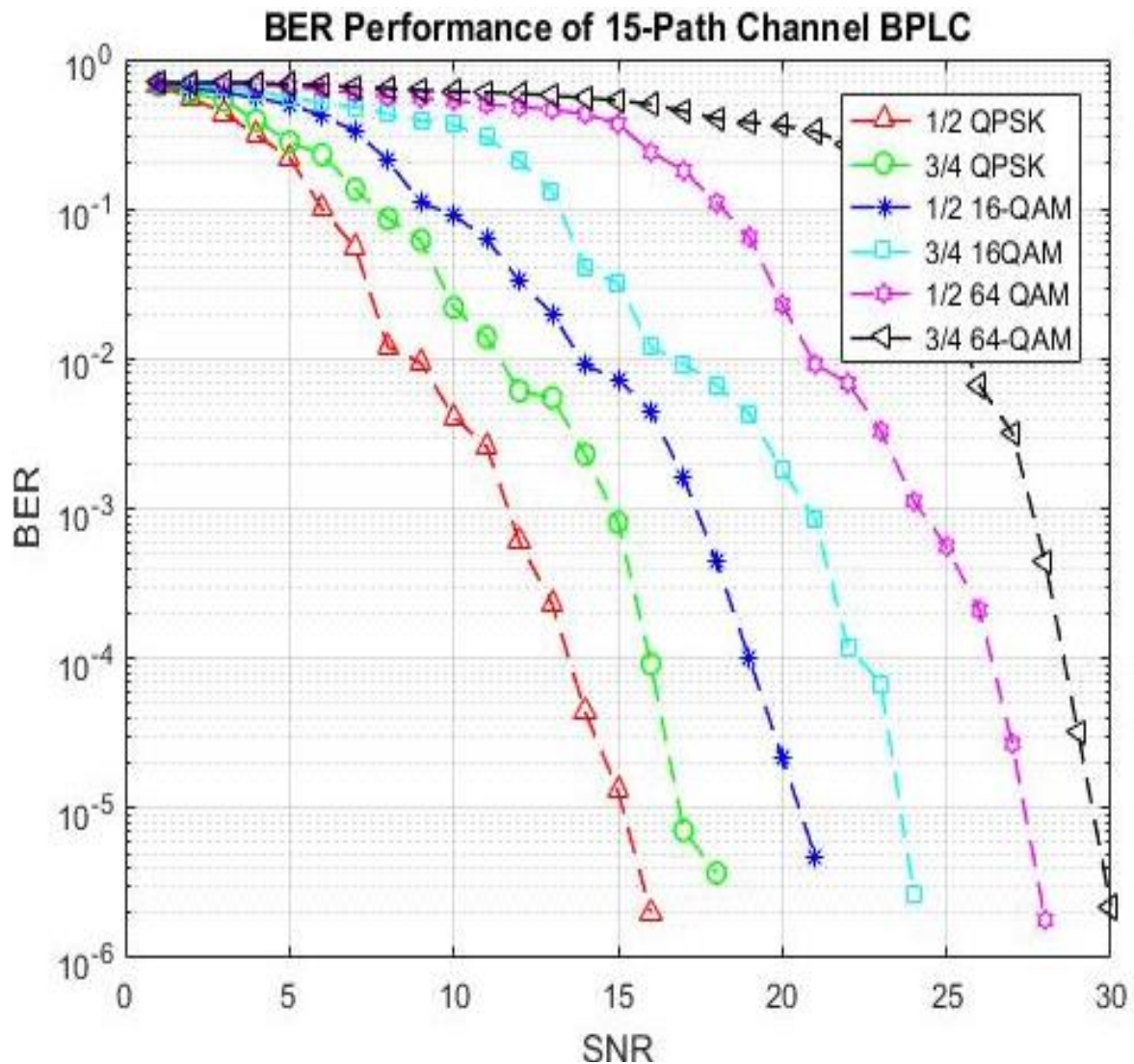


Figure 5.2. 15-path fading channel BER performance

The BER performance of 15-path SISO fading channel is given in Fig. 5.2. As can be seen from the figure, BER performance decreases compared to 4-path SISO channel due to harsh channel environment. Adaptive modulation and coding technique increases BER performance as 4-path channel model. QPSK modulation scheme with $\frac{1}{2}$ coding rate has the performance at the lower SNR values, however, 64-QAM modulation scheme with $\frac{3}{4}$ coding rate performs better than the other constellations at higher SNR values. SNR thresholds are given in the Table 5.1 according to target BER 10^{-3} is achieved.

The BER performances of 2x2, and 3x3 MIMO-PLC communication systems are given in Fig. 5.3 and Fig. 5.4, respectively. As can be seen from both figures, the BER performances are improved by using spatial multiplexing based MIMO communication structure, especially at the higher SNR values.

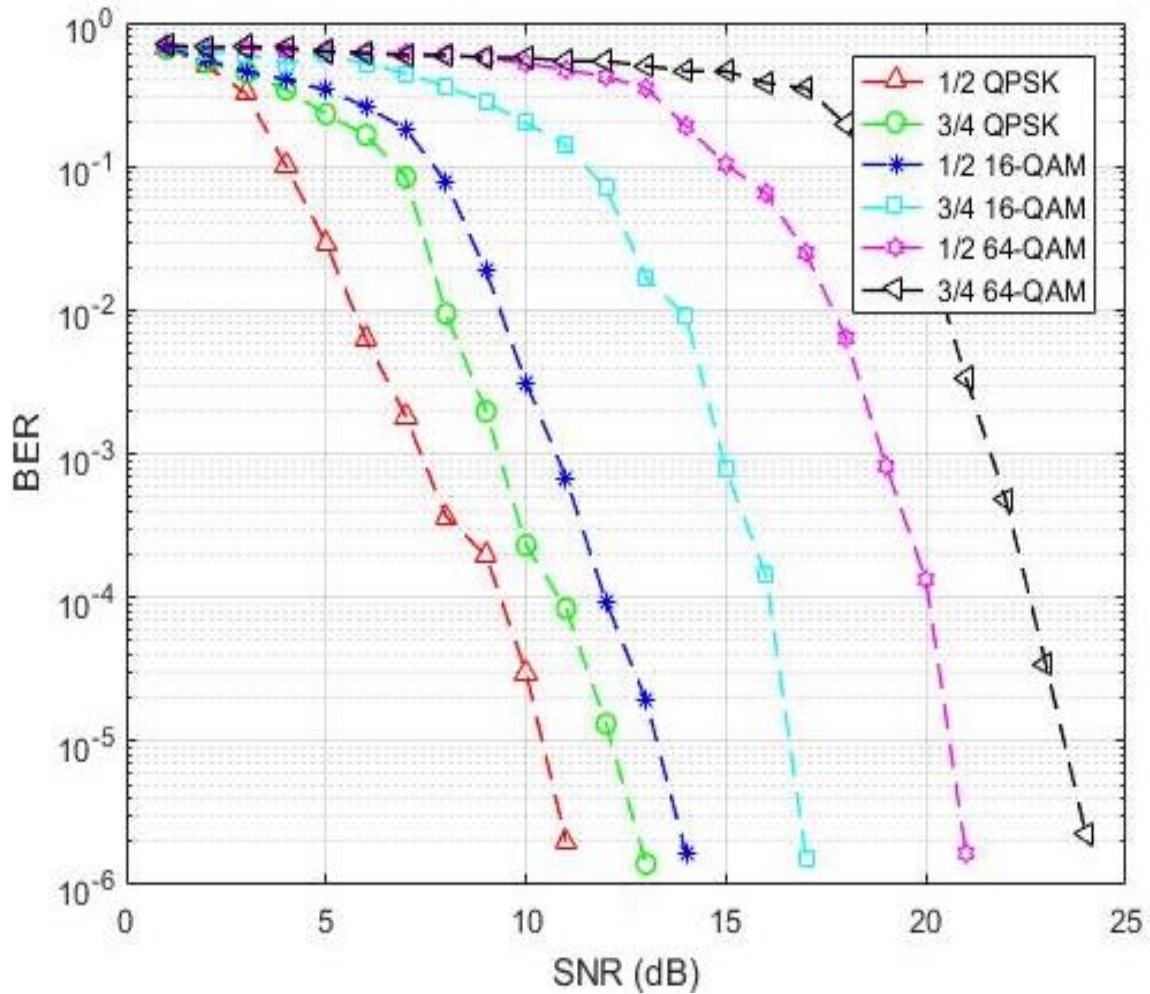


Figure 5.3. BER performance of 2x2 MIMO-PLC

Additionally, adaptive modulation and coding technique improved the BER performances. The lower order modulation scheme with $\frac{1}{2}$ coding rate performed better than the other schemes at the values below 7 dB signal-noise-ratio. By using spatial multiplexing and adaptive modulation coding techniques; it is showed that the BER performance and the channel capacity can be increased.

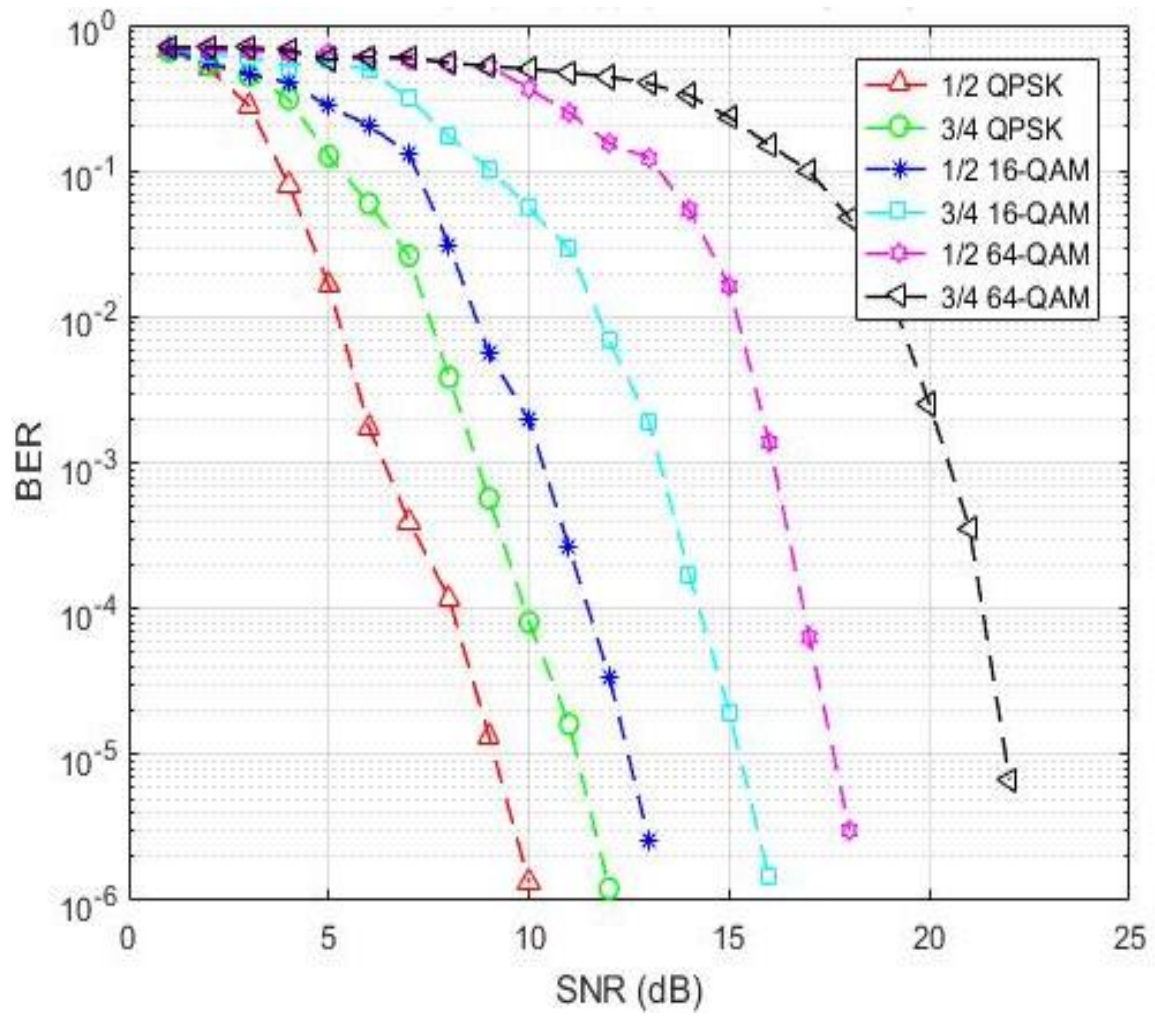


Figure 5.4. BER performance of 3x3 MIMO-PLC

6. CONCLUSION

This thesis examines the bit-error-rate performance analysis of adaptive modulation coding MIMO-OFDM in broadband powerline communication system. We explore the effect of utilizing AMC techniques under highly distorted channel conditions which include multipath fading and impulsive noise. We also examine the effects of multiple-input multiple-output channels in the powerline communication, and also compared MIMO and SISO systems according to their bit-error-rate performances.

To achieve broadband communication and handle with harsh channel conditions such as impulsive noise, fading, and ISI, Orthogonal Frequency-Division Multiplexing modulation technique is utilized. Different modulation orders such as QPSK, 16-QAM, and 64-QAM schemes are used for achieving adaptive modulation and coding. Turbo codes with 1/2 and 3/4 coding rates are used. For decoding, we operated MAP algorithm. Additionally, the powerlines offer more than one channel by having multi-transmission path structure. Thus, we could establish spatial multiplexing based MIMO communication system. We utilize 4-path, and 15-path SISO channel, 2x2 MIMO channel, and 3x3 MIMO channel communication systems. We used Zimmermann's powerline channel model [40] for 4-path and 15-path SISO channel experiments, and we derived 2x2, and 3x3 MIMO powerline channel models by using Tonello and Versolatto's technique [32]. For each channel models, the adaptive modulation and coding technique is carried out by using aforementioned modulation orders and coding rates. The simulation studies are implemented by using MATLAB simulation program.

It is seen from the experiments, the lower modulation orders and coding rates perform better than higher modulation orders and coding rates at low SNR values both in SISO and MIMO communication systems. However, higher modulation order and coding rate can offer higher data rate, but lower bit error rate performance. It is observed that 2x2, and 3x3 MIMO systems perform better than, especially at the higher SNR values, SISO system in the powerline communication. Adaptive modulation and coding technique improved BER performance in the both SISO and MIMO systems as well. High data rates can be achieved by using spatial multiplexing through MIMO channels in such powerline multi-transmission structures.

REFERENCES

1. Anatory, J., Kisakka, M. and Mvungi, N. (2007). Channel model for broadband power-line communication. *IEEE Transactions on Power Delivery*, 22(1), 135-41.
2. Bahl, L., Cocke, J., Jelinek, F. and Raviv, J. (1974). Optimal decoding of linear codes for minimizing symbol error rate (corresp.). *IEEE Transactions on information theory*, 20(2), 284-287.
3. Berger, L. T., Schwager, A., Pagani, P. and Schneider, D. (Eds.). (2014). *MIMO power line communications: narrow and broadband standards, EMC, and advanced processing*. Boca Raton: CRC Press. 89-119.
4. Berrou, C., Glavieux, A. and Thitimajshima, P. (1993). *Near Shannon limit error-correcting coding and decoding: Turbo-codes*. Technical Program, Conference Record, IEEE International Conference on communication, 2, 1064-70.
5. Bolcskei, H., Gesbert D. and Arogyaswami, J. P. (2002) On the capacity of OFDM-based spatial multiplexing systems. *IEEE Transactions on communications*, 50(2), 225-34.
6. Cho, Y. S., Kim, J., Yang, W. Y. and Kang, C. G.. (2010) *MIMO-OFDM Wireless Communications with MATLAB*. Singapore: Wiley. 25-152, 189-209.
7. Coleri, S., Ergen, M., Puri, A. and Bahai, A. (2002) Channel estimation techniques based on pilot arrangement in OFDM systems. *IEEE Transactions on broadcasting*, 48(3), 223-9.
8. Dusan, M. (1998). OFDM as a possible modulation technique for multimedia applications in the range of mm waves. *Introduction to OFDM*, 1, 10-30.
9. Telatar, E. (1995). Capacity of multi-antenna Gaussian channels. *Transactions on Emerging Telecommunications Technologies*, 10(6), 585-95.
10. European PLC Research Alliance. (2005). Theoretical postulation of plc channel model. *In OPERA*, 1–71.
11. Finamore, W. A., Ribeiro, M.V. and Lampe, L. (2012). *Advancing power line communication: Cognitive, cooperative, and mimo communication*. Brazilian Telecommunications Symposium, Brazil, 13-6.
12. Foschini, G. J. and Gans, M. (1998). On limits of wireless communications in a fading environment when using multiple antennas. *Wireless Personal Communication*, 311–35.

13. Foschini, G. J. (1996). Layered space-time architecture for wireless communication in fading environments when using multi-element antennas. *Bell System Technical Journal*, 41–59.
14. Goldsmith, A. (2005). *Wireless Communication*. Cambridge: Cambridge UP, 374-96, 452-96.
15. Philipps, H. (1992). *Modeling of powerline communication channels*. in Proc. 3rd Int. Symp. Powerline Communications and Its Applications, Lancaster, 14–21.
16. Hrasnica H., Haidine, A. and Lehnert, R. (2005). *Broadband Powerline Communications Networks*. Singapore: Wiley.
17. Heath, R. W. and Paulraj, A.J. (2005). Switching between diversity and multiplexing in MIMO systems. *IEEE Transactions on Communications*, 53(6), 962-8.
18. Hendrick C. F., Lampe, L., Newbury, J. and Swart T. G. (2010). *Powerline Communications Networks, Theory and Applications for Narrowband and Broadband Communications over Power Lines*. Singapore: Wiley, 7-119.
19. Hyeon Y. C., Tsuritani, T. and Morita, I. (2012). BER-adaptive flexible-format transmitter for elastic optical networks. *Optics Express* 20, 18652-8.
20. Winters, J. (1987). On the capacity of radio communication systems with diversity in a Rayleigh fading environment. *IEEE Journal on Selected Areas in Communications*, 871–8.
21. Dostert, K. Telecommunications over the Power Distribution Grid-Possibilities and Limitations. *IIR Power line*, 6, 97.
22. Leslie A. B. (1981). Understanding middletons’s canonical formula for class a noise. *IEEE Transactions on Electromagnetic Compatibility*, 23(4), 337-44.
23. Lucian, M. (2013). Turbo Decoding Using BCJR Algorithm. *Journal of Electrical & Electronics Engineering*, 6(1), 87-90.
24. Gotz, M., Rapp, M. and Dostert, K. (2004). Power line channel characteristics and their effect on communication system design. *IEEE Communications Magazine*, 42(4), 78-86.
25. Katayama, M., Yamazato, T. and Okada, H. (2006). A mathematical model of noise in narrowband power line communication systems. *IEEE Journal on Selected Areas in Communications*, 24(7), 1267-1276.
26. Molisch, A. F., Win, M. Z. and Winters, J. H. (2002). Space-time-frequency (STF) coding for MIMO-OFDM systems. *IEEE Communications Letters*, 6(9), 370-2.

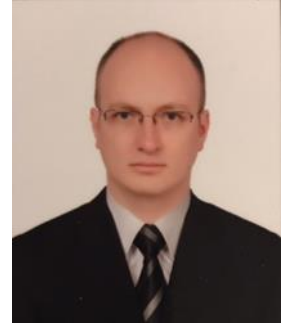
27. Palomar, D. P., Cioffi, J. M. and Lagunas, M. A. (2003). Joint Tx-Rx beamforming design for multicarrier MIMO channels: A unified framework for convex optimization. *IEEE Transactions on Signal Processing*, 51(9), 2381-401.
28. Hashmat, R., Pagani, P., Zeddani, A. and Chonave, T. (2011). *A channel model for multiple input multiple output inhome powerline networks*. 2011 IEEE International Symposium on Power Line Communications and Its Applications (ISPLC), 35-41.
29. Sartenaer, T. and Delogne, P. (2001). *Powerline cables modelling for broadband communications*. In Proc. IEEE Int. Conf. Power Line Communications and Its Applications, 331-7.
30. Shannon, C. E. (1949). Communication in the presence of noise. *Proceedings of the IRE*, 37(1), 10-21.
31. Sun, S., Rappaport, T. S., Heath, R. W., Nix, A. and Rangan, S. (2014). MIMO for millimeter-wave wireless communications: Beamforming, spatial multiplexing, or both?. *IEEE Communications Magazine*, 52(12), 110-121.
32. Tonello, A. M. and Versolatto, F. (2009). *New results on top-down and bottom-up statistical PLC channel modeling*. In Third workshop on power line communications, 1-2.
33. Van de Beek, J. J., Sandell, M. and Borjesson, P. O. (1997). ML estimation of time and frequency offset in OFDM systems. *IEEE Transactions on Signal Processing*, 45(7), 1800-1805.
34. Van De Beek, J. J., Edfors, O., Sandell, M., Wilson, S. K. and Borjesson, P. O. (1995) On channel estimation in OFDM systems. *Vehicular Technology Conference*, 45(2), 815-9.
35. Zou, W. Y. and Wu, Y. (1995). COFDM: An overview. *IEEE Transactions on Broadcasting*, 41(1), 1-8.
36. Yang, B., Letaief, K. B., Cheng, R. S. and Cao, Z. (2001). Channel estimation for OFDM transmission in multipath fading channels based on parametric channel modeling. *IEEE Transactions on Communications*, 49(3), 467-479.
37. Yang, H. (2005). A road to future broadband wireless access: MIMO-OFDM-based air interface. *IEEE Communications Magazine*, 43(1), 53-60.
38. Yoo, J., Choe, S. and Pine, N. (2012). MIMO-OFDM based broadband power line communication using antenna and fading diversity. *IEICE Transactions on Communications*, 95(5), 1822-1825.

39. Yoo, J. and Choe, S. (2012). *MIMO-OFDM based indoor power line communication using spatial diversity coding and MRC schemes*. In Communications (APCC), 2012 18th Asia-Pacific Conference on, 635-40.
40. Zimmermann, M. and Dostert, K. (2002). A multipath model for the powerline channel. *IEEE Transactions on Communication*, 50(4), 553-559.
41. Zimmermann, M. and Dostert, K. (2002). Analysis and modeling of impulsive noise in broad-band powerline communications. *IEEE Transactions on Electromagnetic Compatibility*, 44(1), 249-258.

RESUME

Personal Information

Surname, name : KARAARSLAN, Güray
 Nationality : T.C.
 Date and place of birth : 12.08.1989, Keçiören
 Marital status : Evli
 Phone number : 0 (312) 368 61 39
 e-mail : guray.karaarslan@gmail.com



Education Information

Degree	University	Year
Master	Gazi University Electrical and Electronics Engineering	2015-2018
Bachelor	Erciyes University Electrical and Electronics Engineering	2009-2013

Work Experience

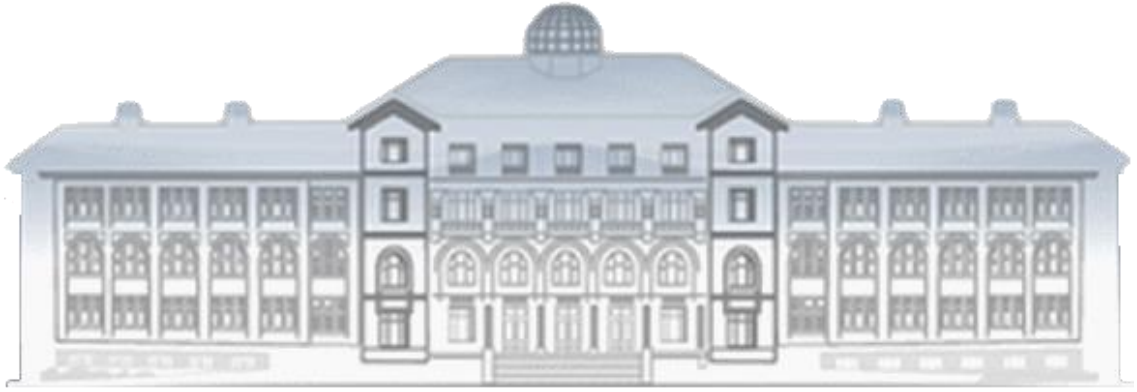
Year	Institution	Position Held
2013-2017	University of Turkish Aeronautical Association	Rsc. Assistant

Foreign Language

English

Publications

Karaarslan, G. and Ertuğ Ö. (2017). *Adaptive Modulation and Coding Technique under Multipath Fading and Impulsive Noise in Broadband Power-line Communication*. Electrical and Electronics Engineering (ELECO), 10th International Conference on, 1430-34.



GAZİ GELECEKTİR..